

**University of Alberta**

**Aggregation and Sedimentation of Fine Solids in  
Non-Aqueous Media**

by

**Amin Karkooti**

A thesis submitted to the Faculty of Graduate Studies and Research  
in partial fulfillment of the requirements for the degree of

**Master of Science**

in

**Chemical Engineering**

**Department of Chemical and Materials Engineering**

©Amin Karkooti  
Spring 2014  
Edmonton, Alberta

Permission is hereby granted to the University of Alberta Libraries to reproduce single copies of this thesis and to lend or sell such copies for private, scholarly or scientific research purposes only. Where the thesis is converted to, or otherwise made available in digital form, the University of Alberta will advise potential users of the thesis of these terms.

The author reserves all other publication and other rights in association with the copyright in the thesis and, except as herein before provided, neither the thesis nor any substantial portion thereof may be printed or otherwise reproduced in any material form whatsoever without the author's prior written permission

## Abstracts

Environmental concerns about water-based extraction necessitate the development of an alternative non-aqueous extraction method. One of the challenges that any non-aqueous extraction process is encountered is the elimination of suspended fine solids from solvent-diluted bitumen. This study focuses on the fundamental science behind the paraffinic froth treatment process to provide a real insight into the role of asphaltenes in removal of unwanted suspended particles from bitumen froth. We examined the aggregation and sedimentation of model solid in mixture of solvents and bitumen or de-asphalted bitumen using a sedimentation balance. The solvents were heptane, toluene or a mixture of the two known as heptol. The model solids were micron-sized bitumen-coated silica particles. In a set of experiments, the effect of aromatic content of the solvents on sedimentation behavior was investigated. The results showed that the sedimentation behaviors of bitumen coated silica particles are highly sensitive to the aromatic content of the organic solvents. The experiments involved quantifying the settling rates of the particles as the aromatic content of the solvent was varied. The results showed that, in addition to being captured by asphaltene networks, the suspended solids could also homo-flocculate and thus form aggregates and be separated in an heptane-diluted bitumen environment. The results indicate that it is possible to control the stability fine particulates in oil, through tuning the aromaticity of the organic solvents.

## Acknowledgement

I would like to take this opportunity to thank my supervisors, Dr. Anthony Yeung and Dr. Qi Liu for giving me the opportunity to work with them. I appreciate their supports and their valuable guidance during this research.

I would like to acknowledge Centre for Oil Sands Innovation (COSI) at the University of Alberta for the financial support of this project.

I would also like to thank my friends and colleagues at the University of Alberta. They helped to make my research experience most enjoyable. My special thanks to Lily Laser for her energetic and kind supports during these years.

And my deepest love and gratitude goes to my family members. I appreciate their unconditional love and support.

# Table of Contents

1	Introduction .....	1
1.1	Oil sands.....	1
1.2	Recovery methods.....	2
1.3	Problem statement.....	3
1.4	Objective of present research.....	7
1.5	Thesis structure.....	9
2	Theoretical background.....	10
2.1	Sedimentation.....	10
2.2	Aggregation phenomena.....	13
2.3	Structure of aggregates.....	14
2.4	Mechanism of aggregation.....	16
2.5	Kinetics of aggregation.....	17
2.5.1	Collision frequency $\beta_{ij}$ .....	17
2.5.2	Collision efficiency $\alpha$ .....	18
2.6	Inter-particle forces in liquid media.....	19
2.6.1	Inter-particle forces in aqueous media.....	20
2.6.2	Columbic interaction .....	20
2.6.3	Van der Waals attraction.....	20

2.6.4	Electric double layer repulsion.....	21
2.6.5	DLVO theory .....	23
2.6.6	Inter-particle forces in non-aqueous media .....	23
2.6.7	Steric repulsion.....	24
2.6.8	Cross bridging .....	25
2.7	Particles size measurements method.....	25
2.8	Settling rate measurement methods.....	27
2.8.1	Optical methods.....	27
2.8.2	Ashing technique.....	28
2.8.3	Sedimentation balance .....	29
2.8.4	X-ray method for detection of the settling solids.....	30
2.8.5	In line monitoring methods.....	31
3	Material and method .....	32
3.1	Solvents.....	32
3.2	Silica particles.....	32
3.2.1	Clean silica.....	32
3.2.2	Bitumen-coated silica .....	33
3.3	Preparation of bitumen coated silica.....	33
3.4	Sample preparation for settling tests.....	34
3.5	Preparation of de-asphalted bitumen.....	35

3.6	Settling rate measurement.....	36
4	Results and discussion .....	39
4.1	Particle size distribution measurement:.....	41
4.2	Sedimentation in water:.....	43
4.3	Sedimentation in organic solvents:.....	44
4.4	Effect of oil phase composition on solids settling rate.....	46
4.5	Settling rate.....	50
5	Summary and recommendation .....	60
6	References: .....	63

## List of Figures

Figure 1.1 Schematic of the Non-aqueous bitumen extraction process.....	6
Figure 2.1 Sedimentation of concentrated suspensions (a) Type 1 settling,.....	13
Figure 2.2 Fractal shape of aggregates: (A) loose structure, and (B) packed structure[28]. .....	15
Figure 2.3 large molecules adsorption on the surface in .....	24
Figure 2.4 Polymer cross bridging between two particles.....	25
Figure 2.5 (a) Schematic of the settling experiment. Samples were taken from a fixed location 1 cm from the free surface. (b) Typical plot of solids content in the sample versus time[17].....	29
Figure 2.6 In-line experimental setup.....	31
Figure 3.1 Sample preparation procedure in a Teflon bottle .....	35
Figure 3.2 A schematic of sedimentation experimental set up, b) a.....	37
Figure 4.1 A) Clean silica particles B) Bitumen-coated silica particles.....	39
Figure 4.2 Particle size distribution of clean silica particles in water .....	41
Figure 4.3 Particle size distribution of treated silica particles in toluene .....	42
Figure 4.4 Sedimentation behavior of clean silica particles in water with pH 6.8 and pH 2 .....	43
Figure 4.5 Sedimentation behavior of clean silica particles in water with pH 2 ..	44

Figure 4.6 Sedimentation behavior of clean silica and treated silica particles in pure toluene .....	45
Figure 4.7 Sedimentation behavior of clean silica particles in pure toluene .....	46
Figure 4.8 Sedimentation behavior of treated silica in toluene and heptane + 3% de-asphalted bitumen .....	47
Figure 4.9 Bitumen-coated solid particles in (a) a paraffinic solvent, .....	48
Figure 4.10 Sedimentation behavior of treated silica in heptane + 3% de-asphalted .....	50
Figure 4.11 Effect of addition of 3 wt. % maltene on the settling rate of bitumen-treated silica in heptol (a mixture of toluene and n-heptane). The dotted blue line is the expected settling rates below 50 vol. % toluene content in heptol. ....	51
Figure 4.12 Possible mechanisms for paraffinic froth treatment: a) asphaltene ...	54
Figure 4.13 The settling curve for Case A) bitumen-coated silica particles in 3 wt. % diluted maltene, Case B) precipitated asphaltenes in 4.5 wt. % diluted bitumen (no silica particle) and Case C) bitumen-coated silica particles in 4.5 wt. % diluted bitumen; collecting tray is located at depth of 15 mm. ....	56
Figure 4.15 The settling curve for Case A) bitumen-coated silica particles in 3 wt. % diluted maltene, Case B) precipitated asphaltenes in 4.5 wt. % diluted bitumen (no silica particle) and Case C) bitumen-coated silica particles in 4.5 wt. % diluted bitumen; collecting tray is located at depth of 30 mm. ....	58

## List of Tables

Table 4.1 Solids and the corresponding hydrocarbon phases that were studied. ..	40
Table 4.2 Median particle size of samples used in the experiments. ....	42
Table 4.3 Calculated settling time and observed settling time in different hydrocarbon used in the experiment. ....	48

## Nomenclature

m Mass (kg)

t Time (s)

Q Magnitude of electric charge (C)

D distance (m)

R Radius (m)

A Hamakar constant (J)

$V_s$  Particle settling velocity (m/s)

d Hydrodynamic diameter (m)

g Gravitational acceleration ( $\text{m/s}^2$ )

l Length of centrifugal tube (m)

F Force (N)

$\rho_p$  Density of particles ( $\text{kg/m}^3$ )

$\rho_f$  Density of fluid ( $\text{kg/m}^3$ )

$\mu$  Fluid viscosity (Pa.s)

G Mean shear rate

V Volt

# 1 Introduction

## 1.1 Oil sands

The Canadian oil sands, with 174 billion barrels of recoverable oil, is one of the largest petroleum resources in the world [1]. Oil sands are primarily, a mixture of bitumen, sands, clays and salty water. Oil sands deposits in Canada locate in the Athabasca basin of north-eastern Alberta and Saskatchewan, occupying a total area of 149,000 square kilometers [2]. The primary value in oil sands is the bitumen which is high molar mass petroleum, characterized by very high viscosities, high densities, relatively high heavy metal concentrations and a low ratio of hydrogen to carbon in comparison with conventional oil [2]. Steadily rising market price for crude oil, growing uncertainty about the global supply of oil and rapidly growing global demand lead to increase the importance of oil sands [3]. At present, Canada's oil sands is regarded as an abundant, secure and affordable source of crude oil. In Alberta, the current operations are largely situated in three main areas: the Athabasca, the Peace River and the Cold Lake areas.

Oil sands usually consist of 8-12 wt.% bitumen, 80-85 wt.% solids, and 5-6 wt.% formation water [2]. Bitumen is a mixture of a very large number of components and it is not practical to classify its components by their chemical composition. Bitumen is often characterized chemically by its hydrocarbon class compositions, such as the saturates–aromatics–resins–asphaltenes (SARA) contents [4].

Asphaltenes are a solubility class defined as insolubles in light aliphatic solvent (e.g., n-pentane or n-heptane) and solubles in aromatic solvent (e.g., toluene).

The extracted raw bitumen from oil sands must be refined and upgraded before it can be used as fuels or other petroleum-derived products.

## 1.2 Recovery methods

The methods that have been used to recover oil sands depend on the depth of the oil sands deposit. Deeper deposits are accessed through various in situ technologies (e.g., steam-assisted gravity drainage, SAGD, VAPEX), while mining the ore is practical when the oil sands deposit is close to the surface (the depth less than 75 m beneath the ground) [2].

In steam-assisted in-situ recovery, steam and solvent are injected into horizontal well drilled through the oil sands deposit to increase the temperature and reduce the viscosity of bitumen. Under the gravity, the less viscous bitumen flows to the production well where it is transported to the surface [2].

In open pit mining, the overburden on the top of the deposit is first removed. The ore is then mined with shovels and transported to the bitumen extraction site. Next, the oil sands ore lumps are crushed to smaller sizes and mixed with warm water and chemical additives (e.g. caustic soda) to form an oil sand slurry. In this process, bitumen dislodges from the sand grains. To promote liberation of bitumen, mechanical energy in the form of agitation or pipeline transport is introduced into the slurry. Simultaneously, air is injected into the slurry to aerate the bitumen droplets. Due to buoyancy effects, the liberated, aerated bitumen floats to the top of the gravity separation vessel and forms a froth layer which can

be easily collected from the top of the vessels. The collected bitumen froth contains roughly 60 wt.% bitumen, 30 wt.% water and 10 wt.% solids [5]. The froth must be purified further in the next process, referred to as froth treatment, to eliminate the unwanted water and solids from bitumen. After froth treatment, the bitumen content is usually more than 99% by weight, so it is ready to be sent to upgrading units. For the time being, the majority of raw bitumen in Alberta is produced by mining the ore, followed by a water-based extraction process.

### **1.3 Problem statement**

Although oil sands industries have clear economic benefits, its environmental footprints are not negligible. The main concerns related to water-based bitumen production today include: how much water the industry consumes, the volume of toxic tailings waste produced, and the greenhouse gas and air pollution emitted. This process requires withdrawal of considerable amount of fresh water from rivers for different purposes, such as separation of bitumen from sand and utility functions. Knowing this fact, there are serious environmental issues related to the current “water-based” bitumen extraction method. Our particular concern here is the consumption of large volumes of water by water-based process, which is the direct cause of the following environmental problems[3], [6]:

- Oil sands extraction consumes large amounts of water, despite current recycling efforts. The Athabasca River provides fresh water for the industry, as well as the city of Fort McMurray and neighbouring communities. In 2011, oil sands operators used approximately 170 million cubic metres of water, equivalent to the residential water use of 1.7 million

Canadians, or roughly the amount of water used by everyone living in Calgary and Edmonton combined [6]. The current rate of water consumption is already raising concerns about its negative impact on these communities and the health of people living in the vicinity of oil sands development and the integrity of nearby ecosystems.

- The oil sands extraction process consumes large amounts of energy, derived from coal-based power, natural gas, and diesel fuel. Water has a large heat capacity and the heating of the process water, especially during winter, needs massive amounts of thermal energy to heat the water (up to 80°C). This fact causes the oil sands to be considered as the largest contributor to greenhouse gas emissions in Canada [3].
- Tailings are a waste by-product of the oil sands mining extraction process that consists of water, clays, sand and residual bitumen, along with various salts, heavy metals and other compounds that can be toxic if concentrations are sufficiently high. This contaminated water cannot be released back into the Athabasca River; it is instead contained in large tailings ponds. These ponds currently cover 176 square kilometres of the landscape, and contain 830 million cubic metres of tailings waste [6]. There remains considerable uncertainty as to whether the tailings ponds can be reclaimed to a level that sustains functional ecosystems equivalent to those that were in existence prior to mining. It can also potentially be the cause of large scale environmental pollution through leakage of contaminants into the soil and water aquifers or surface water.

In 2012, the oil sands industry produced 1.9 million barrels of bitumen each day. A decade from now, total bitumen production is projected to reach 3.8 million barrels per day, and the Canadian association of petroleum producers expects the industry will surpass 5 million barrels a day by the end of 2030 [6]. The intensity of water consumption in oil sands industry, particularly in light of new goal for production expansion by 2030, must be urgently addressed before the above-mentioned problems progress to a point where the future of the oil sands industry to be under threat.

Considering above mentioned concerns, development of an alternative method seems to be a necessity. We believe solvent-based (or non-aqueous) extraction technology may assist the Canadian oil sands industry to disengage from water-based processes. The basic principles of such a non-aqueous technology are simple: Mined oil sands are first mixed with an organic solvent in which bitumen is soluble. Then, the mixture passes through a large-sand-grain separation stage. In this stage, the separation can be accomplished via conventional methods such as sedimentation, centrifugation or filtration. After eliminating coarse solids, the product stream contains diluted bitumen. The solvent in the product stream can be recovered through a distillation process and be recycled back to mix with new mined oil sands. Following this, the extracted bitumen is sent to upgrade into synthetic crude oil. An abstract representation of such a process is shown in Figure 1.1.

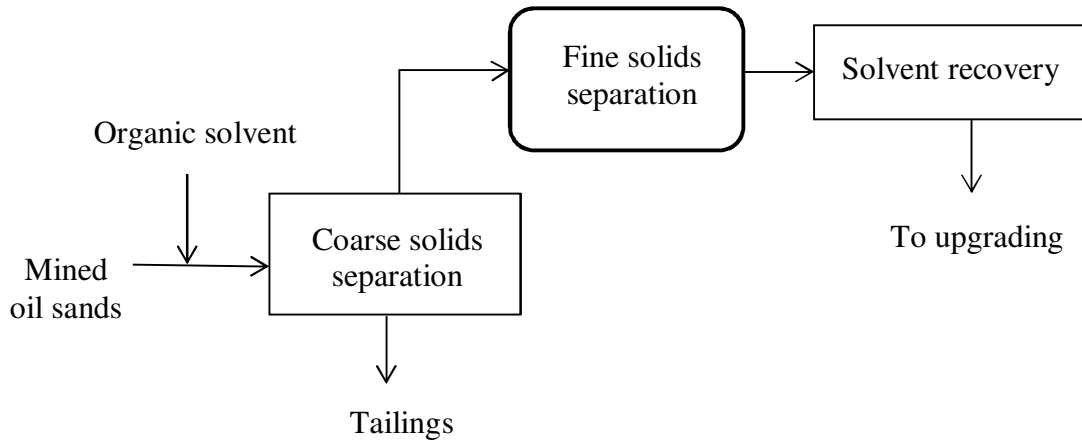


Figure 1.1 Schematic of the Non-aqueous bitumen extraction process

In the past several decades, some non-aqueous processes had been put forward for bitumen extraction[7]–[15], Unfortunately, none of these methods had advanced further than pilot stages.

The failure of those processes could be attributed to two main setbacks:

- Inability to remove the fine solids that are suspended in the diluted bitumen.
- Inability to recover the residual oil and solvent that was trapped within the small crevices between the sand grains.

The first challenge leads to corrosion in the pipelines, fouling on the catalysts, and plugging the packed beds in downstream. The latter problem can result in solvent loss and large scale environmental pollution. To develop a feasible non-aqueous extraction technology, it is essential to find a solution for the above mentioned obstacles before putting any commercial plan into practice.

## 1.4 Objective of present research

This research is motivated by the first problem, the removal of unwanted fine solids from a diluted bitumen medium. These fine particles are mainly in the range of 10 nm to 10  $\mu\text{m}$ . The removal of these particles using conventional methods, such as centrifugation and filtration, is expensive and ineffective on the commercial scale. However, if one could find suitable conditions under which the fine particles destabilized and formed big clusters, then sufficient density difference between aggregate and suspending liquid would permit implementation of simple gravity settling. One of the primary objectives of this study is to find the optimum conditions for the aggregation (i.e. destabilization) of particles in diluted bitumen, which in turn will facilitate removal of these impurities.

Recently, it was discovered accidentally that, during froth treatment, replacement of naphtha with a paraffinic solvent as diluent can cause the majority of the suspended fine solids to aggregate. As a result, removal of particulates is possible by simple gravity settling. This is the so-called paraffinic froth treatment (PFT) process. Many studies have been conducted on this process, which can produce solids- and water-free diluted bitumen. To a certain degree, this PFT process is similar to what one would expect to see during solvent-based extraction. However, the mechanism behind this PFT process is still unknown. Based on the common belief in the literature, asphaltene molecules will precipitate in a paraffinic solvent and form a network; all unwanted particulates (fine solids and emulsified water) will irreversibly be trapped by the asphaltene network, which results in the separation process [16].

The main question is: how will precipitation of asphaltenes affect the entrapment of solids? In an earlier study, we have demonstrated that in pure paraffinic solvents (such as *n*-heptane), bitumen-coated solids would homo-aggregate amongst themselves simply through van der Waals attraction [17]. This evidence suggests homo-aggregation of solids as an effective parallel mechanism happening in PFT. It is not evident, for example, whether the “floc networks” which result from asphaltenes aggregation are responsible for entrapping and collecting all water droplets and fine solids in the hydrocarbon medium. In the absence of emulsified water, is the PFT process capable of aggregating and removing suspended fine solids, or is water crucial as a “collector” of the mainly hydrophilic fine solids?

To improve the separations technology, study of the mechanisms behind aggregation and sedimentation of fine particles in non-aqueous (i.e. organic) liquids seems essential.

In this thesis, it is our aim to uncover the fundamental mechanism(s) that govern the sedimentation of solid particles in non-aqueous suspensions (i.e. in diluted bitumen).

An understanding of the basic mechanisms of aggregation will provide valuable information in efforts to remove the fine particles more efficiently. This study will provide insight into the mechanism behind the paraffinic froth treatment process.

## 1.5 Thesis structure

This thesis is organised into the following chapters:

Chapter 2 will provide background information on the basics of sedimentation.

Chapter 3 covers experimental approaches that are used to study the physics of particle aggregation. In this approach, a sedimentation balance is used to determine the settling rate of silica particles in water of different pH, and in organic solvents with different aromatic contents. Also, the relation between particle settling rate and the presence/absence of asphaltenes in suspension is studied. The experimental results and discussion on the settling mechanisms in non-aqueous media are provided in Chapter 4. And finally, the contributions of this research and suggestions for future work are discussed in Chapter 5.

## 2 Theoretical background

As mentioned in Chapter 1, the main obstacles in solvent-based bitumen extraction is the elimination of suspended fine solids in the oil phase (i.e. diluted bitumen); this is to prevent further problems downstream, such as corrosion in the pipelines, fouling on the catalysts and plugging the packed beds in the upgrading units. In the separation process, conventional separation methods (e.g. sedimentation, filtration or centrifugation) can be implemented for large sand grains. However, a considerable amount of ultra-fine particles remain in the bitumen froth and are not easy to remove. These ultra-fine particles, with major dimensions of  $< 1 \mu\text{m}$ [2], can unfavorably affect the separations process and quality of bitumen through complex interactions with components of the oil phase.

To improve the separations technology, study of the mechanisms behind aggregation and sedimentation of fine particles in non-aqueous (i.e. organic) liquids seems essential. Therefore, the basic concepts of sedimentation, along with fine particles interactions (with one another and with bitumen components) will be discussed in this chapter.

### 2.1 Sedimentation

Gravity sedimentation is the simplest and cheapest form of separation processes. Suppose an isolated particle (the dense phase) is moving through a fluid (the light phase) in a gravitational field. The particle has the tendency to settle out of fluid

in response to the forces (i.e. frictional, gravitational forces) acting on it. This is called the sedimentation process.

Stokes sedimentation theory describes the steady-state or terminal velocity of particles as a function of their size and mass in a gravitational field. The terminal velocity of a single particle is reached when all the exerted forces come to balance. The terminal velocity can be calculated by Stokes law for a single isolated spherical particle in laminar flow[18]:

$$V_s = \frac{d^2 g (\rho_p - \rho_f)}{18\mu} \quad (2-1)$$

Here,  $V_s$ ,  $d$ ,  $\rho_p$ ,  $\rho_f$  and  $\mu$  represent accordingly the particle settling velocity, the hydrodynamic diameter of the particle, the density of the particles, the density of the fluid, and the fluid viscosity.

The sedimentation behaviour of a suspension depends on concentration. In a dilute suspension, particles settle independently and their motion is not influenced by the motion of other particles. In more concentrated suspension, however, sedimentation is affected by other particles and zone settling (hindered settling) is observed [19]. In a concentrated suspension, significant interaction between particles increases the effective frictional forces and hinders the settling of particles. As a consequence, the sedimentation rate of a particle in a concentrated suspension is slower than the isolated particles (with little or no mutual interference amongst particles).

Previous studies[20]–[23] on this subject show that particles in concentrated suspensions may settle in one of the two following ways. Type 1 settling, as shown in Figure 2.1a, has four zones and is more common in practice. Initially,

aggregation of fine solids leads to a brief accelerated settling of the suspension, and then a clear liquid zone appears on the top (zone A). The interface between the clear liquid and the rest of the suspension moves downward in a more-or-less constant rate, and zone B — called the hindered or settling zone — appears. In zone B, particles with a strong tendency to aggregate (come together and form a larger unit) do so and settle as a unit. To be precise, individual particles within the aggregate matrix remains in fixed positions relative to each other and settle at the same velocity. Larger particles accumulate at the bottom of the jar and form a sediment layer (zone D). As settling continues, zone B becomes smaller until it eventually disappears, and the upper interface (between zones A and B) reaches the lower interface (between zones B and D). At this point, a direct interface is formed between clear liquid and sediment layer. Later on, further sedimentation results from consolidation of the sediment layer at the bottom, which occurs under the compression settling regime. The compressive forces resulted from the weight of suspension column on the top of the sediment layer, forcing the liquid (in sediment layer) upward and form a loose bed of particles (zone C)[23],[19].

The second type of sedimentation, which is less common in concentrated suspensions, is shown in Figure 2.1b. This is the type of sedimentation when the particle size range is very large. In this case, bigger particles settle faster and leave the smaller ones behind, resulting in the formation of a zone of variable composition (zone C). The sedimentation rate progressively decreases during the whole process because there is no zone of constant composition, and zone C extends from the top interface to the layer of sediment. Generally, it is very

difficult to characterize the sedimentation rate of a suspension of fine particles due to the large number of factors affecting the process. Although a number of empirical equations are available for this purpose[24],[20], they mostly are limited to some specific conditions and the range of their applicability is very narrow.

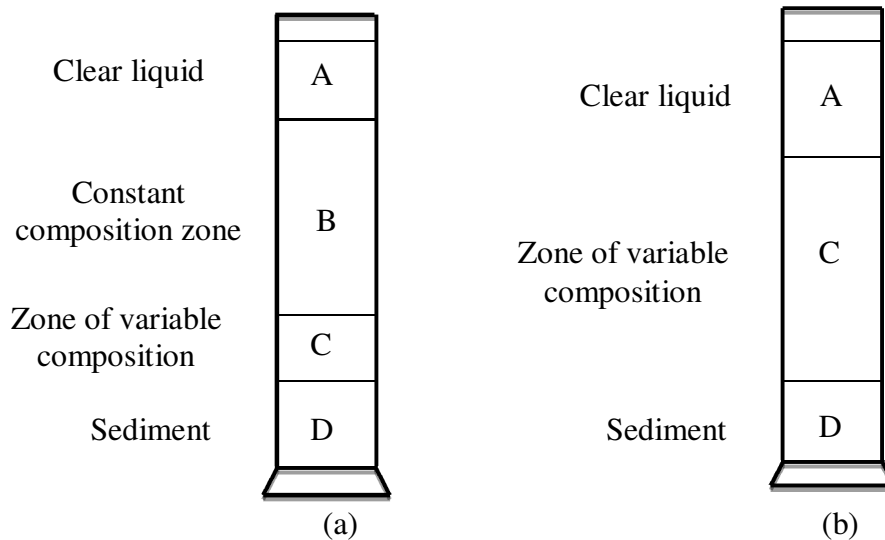


Figure 2.1 Sedimentation of concentrated suspensions (a) Type 1 settling, (b) Type 2 settling

## 2.2 Aggregation phenomena

Aggregation is a process in which two or more particles combine together to form a larger one. As the aggregation process continues, larger clusters form. Aggregation occurs only if particles collide with each other and can adhere when they come into contact, which could be termed as transport and attachment steps. The role of aggregation is extremely important in the process of fine particle separation. When the size of the clusters increase, the settling velocity of the

clusters increases as well. In addition, properties such as density and hydrodynamic radius change during aggregation, which significantly affect the settling rate. In the absence of aggregation, the type of suspending liquid (the hydrocarbon solvent) has only a very minor effect on the settling rate (e.g. Stokes velocity), as fluid properties such as density or viscosity do not vary significantly. However, in reality, the choice of solvent is extremely important as it has very strong effects on the aggregation of the fine solids.

### 2.3 Structure of aggregates

As discussed earlier, particle aggregation provides a way to separate colloids from suspension. In the aggregation process, the particles form self-similar structures called fractal clusters [25]. As illustrated in Figure 2.2, the fractal-shaped aggregates contain hundreds or thousands of primary particles. Depending on whether the aggregation is fast or slow, the shape of clusters will change. To describe the shape of an aggregate, we first need to define fractal dimension as follows[19]:

For a solid object, the mass  $m$  is proportional to the third power of its characteristic length  $L$  :

$$m = L^3 \tag{2 - 2}$$

However, for fractal objects, the exponent is less than 3. The mass of a fractal object scales as

$$m = L^{d_f} \tag{2 - 3}$$

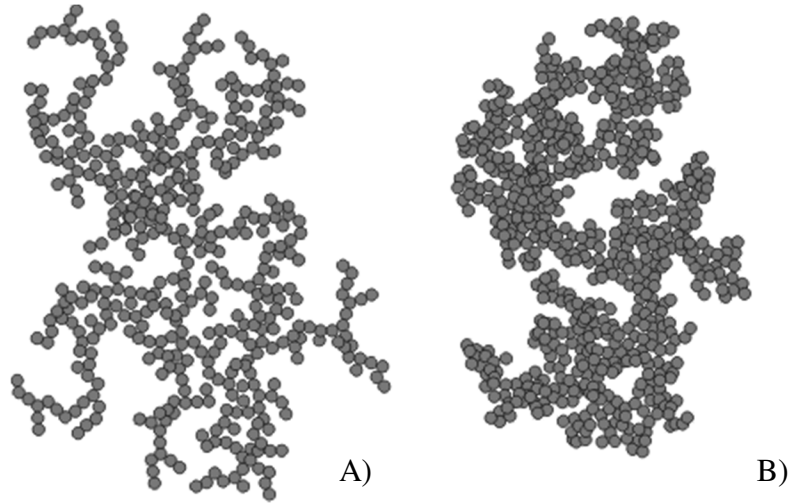


Figure 2.2 Fractal shape of aggregates: (A) loose structure, and (B) packed structure[28].

where  $d_f$  is the fractal dimension in the range of 1 (for linear structure) to 3 (for solid objects); a denser packed aggregate has a higher fractal dimension. It is reported in literature that the fractal dimensions for rapid aggregation is between 1.6 and 1.9, and for slow aggregation, between 2 and 2.3[26].

If single particle addition is the mechanism of aggregate formation, the produced clusters are more compact and have the shapes that are closer to spheres. For the cluster-cluster aggregation, the resulting clusters are usually more loose and tend to grow very rapidly.

When  $d_f = 3$  the equation (2-1) applies for calculating the terminal velocity of single spherical particle while for  $d_f < 3$ , the Stokes equation modified to equation (2-4) [27]:

$$V_s = \frac{d_0^2 g (\rho_p - \rho_f)}{18\mu} \left(\frac{d}{d_0}\right)^{d_f-1} \quad (2 - 4)$$

Here,  $V_s$ ,  $d$ ,  $d_0$ ,  $\rho_p$ ,  $\rho_f$  and  $\mu$  represent accordingly the particle settling velocity, the hydrodynamic diameter of the particle, component particle diameter, the density of the particles, the density of the fluid, and the fluid viscosity.

## 2.4 Mechanism of aggregation

The formation of aggregates originates from collisions of particles. It is generally accepted that there are three mechanisms which cause particles to collide [19], [26], [29]:

- Brownian motion (perikinetic aggregation)
- Velocity gradient (orthokinetic aggregation)
- Differential settling

Brownian motion is the random movement of colloidal particles in a fluid, which can bring two particles together via diffusion. The next mechanism, velocity gradient, resulted from fluid motion which causes particles to acquire different velocities and collide with one another. Finally, differential settling occurs when larger aggregates settle faster than smaller ones; such relative motion can lead to particles collisions.

In our study, velocity gradient does not exist. Therefore, collision between particles will result only from Brownian motion and differential settling. Brownian motion is often the dominant mechanism of transport for colloidal (i.e. sub-micron) particles. As the aggregates grow in size, however, differential settling gradually becomes the more important transport mechanism.

## 2.5 Kinetics of aggregation

Based on the Smoluchowski theory [26], the binary collision frequency  $f_{ij}$  between type- $i$  and type- $j$  particles is given by:

$$f_{ij} = C_{ij} \cdot n_i \cdot n_j \quad (2 - 5)$$

In this equation,  $f_{ij}$  represents the total number of collisions between two particles in a unit volume per unit time, with  $n_i$  and  $n_j$  being the number concentrations of the two particle types. The term  $C_{ij}$  is a constant:

$$C_{ij} = \alpha \cdot \beta_{ij} \quad (2 - 6)$$

where,  $\alpha$  is the collision efficiency and  $\beta_{ij}$  the collision frequency. A collision frequency  $\beta_{ij}$  is due to the transport of particles, and the collision efficiency  $\alpha$  is the probability of forming an aggregate as two particles brought together by collision. These two factors are usually approached separately to simplify the analysis.

### 2.5.1 Collision frequency $\beta_{ij}$

The collision frequency, represented by the symbol  $\beta_{ij}$ , is a parameter reflecting how frequently particles of size  $i$  collide with particles of size  $j$ . It depends on the physical environment such as temperature, viscosity, shear rate and the sizes of the particles, but is independent of the short-range colloidal forces. For simple cases, with the particles considered spherical, the collision frequency is calculated as follows[19], [26], [29]:

Perikinetic: 
$$\beta_{ij} = \frac{2}{3} \frac{k_B T}{\eta} (d_i + d_j)^2 / d_i d_j \quad (2 - 7)$$

$$\text{Orthokinetic: } \beta_{ij} = \frac{G}{6} (d_i + d_j)^3 \quad (2 - 8)$$

$$\text{Differential settling: } \beta_{ij} = \frac{\pi g}{72\eta} \Delta\rho (d_i + d_j)^3 (|d_i - d_j|) \quad (2 - 9)$$

In the above expressions,  $d_i$  and  $d_j$  stand for the diameters of type- $i$  and type- $j$  particles,  $k_B T$  is the thermal energy,  $\eta$  is the viscosity of the surrounding fluid,  $G$  is the mean shear rate due to mechanical agitation,  $\Delta\rho$  is the density difference between the particle and the fluid, and  $g$  is the acceleration due to gravity.

By comparing the general trends of the above equations, we can say that perikinetic collision is determined by the size ratio but not the absolute size of the particles. For the orthokinetic and differential settling cases, there is a strong size-dependence —roughly  $\sim d^3$  in the case of orthokinetics and  $\sim d^4$  in the case of differential settling. Therefore, we would conclude that Brownian motion is predominant for submicron particles; the growth of medium-size aggregates is dominated by orthokinetic effects; and differential sedimentation may become dominant for even larger particles (i.e. larger aggregates, with their faster settling velocities, catch up to smaller aggregates and make contact).

### 2.5.2 Collision efficiency $\alpha$

If all collisions lead to an irreversible aggregation, the rate of aggregation would be equal to the collision rate. In reality, however, as a result of interaction barriers, only a fraction of all the collisions result in formation of aggregate. The collision efficiency, represented by the symbol  $\alpha$ , is defined as

$$\alpha \equiv \frac{\text{number of collisions resulting in aggregation}}{\text{total number of collisions}}$$

In other word, the collision efficiency is the probability that a pair of colliding particles form a permanent aggregate. The collision efficiency is often assumed to be size independent, but it should depend strongly on the inter-particle forces.

Aggregation is not possible if strong repulsion exists between the particles (in such a case,  $\alpha$  is equal to zero). In other words, the collision efficiency approaches unity when there is strong attraction between particles such that they are likely to stick to each other on contact. The collision efficiency thus needs to be included in the rate expressions as discussed above.

The relationship between interparticle forces enables us to predict the collision efficiency. However, it is very complicated to determine this factor under all conditions because it is affected in different ways by different colloidal interactions.

## **2.6 Inter-particle forces in liquid media**

As the particles come into close contact during collision, they can feel attractive and/or repulsive forces that are between the particles. These forces govern the important properties of solids suspensions. Colloidal interactions have two major effects on the aggregation process: first, they have a direct effect on the collision efficiency. If strong repulsion exists between the particles, the collision efficiency will be very low and aggregation will occur only very slowly. In other words, the stability of suspended particles against aggregation is controlled by colloidal forces. The other important notion is the effect of colloid interactions on the

strength of the aggregates; this property will determine whether the aggregates would break up under hydrodynamic shear forces.

In the following pages, the forces that play important roles in aqueous media are discussed.

### **2.6.1 Inter-particle forces in aqueous media**

#### **2.6.2 Columbic interaction**

Columbic interactions result from electrostatic interaction between two charged particles. Two like charges repel each other and unlike charges, in contrast, cause attraction. The Coulomb force between two immobile point charges, separated by a distance  $R$  in free space, is given by[30]

$$F = \frac{Q_1 Q_2}{4\pi\epsilon_0 R^2} \quad (2 - 10)$$

Here,  $Q_1$  and  $Q_2$  are the magnitudes of charges and  $\epsilon_0$  is the permittivity of free space with the value of  $8.854 \times 10^{-12} \text{ C} \cdot \text{V}^{-1} \cdot \text{m}^{-1}$  in SI units.

#### **2.6.3 Van der Waals attraction**

The universal attractive force between any two point particles, such as atoms and molecules, is known as the van der Waals force. Such forces also operate between macroscopic objects and play a very important part in the attraction of colloidal particles. It consists of three different types of dipole-dipole interactions [31]:

- Permanent dipole- permanent dipole interaction (Keesom forces)
- Permanent dipole- induced dipole interaction (Debye forces)

- Induced dipole- induced dipole interaction (London dispersion forces)

The total van der Waals force is the sum of these three terms. The van der Waals interaction is always attractive. The magnitude of the attractive force between macroscopic particles depends on the particles size, the distance between them, and the composition of the particles. The van der Waals force between two spheres of radii  $R_1$  and  $R_2$  is equal to

$$F_{VDW}(r) = -\frac{AR_1R_2}{(R_1+R_2)6r^2} \quad (2 - 11)$$

Here,  $r$  is the distance between the spheres and  $A$  is the effective Hamaker constant which is related to the properties of the interacting bodies and the medium. The inverse dependence of the interaction force on the separation distance and the direct dependence on particles size is notable.

#### 2.6.4 Electric double layer repulsion

When particles are immersed in an aqueous environment, they bear surface charges due to ionization of surface groups. The presence of charged surfaces disturbs the electro-neutrality of the electrolyte solution in the immediate vicinity of the charged surfaces; as a result they change the distribution of nearby ions. Ions of opposite charge (counter-ions) are attracted towards the surface via Coulombic forces, resulting in a higher concentration of counter-ions near the particle surface, while ions of like charge (co-ions) are repelled from the surface. As a consequence of the attraction and repulsion between the ions in the electrolyte solution, two layers of charges are formed around the object.

The first layer, the so-called Stern layer, is part of counter-ion charges located close to the particle surface, while the like charge ions are distributed more broadly in the second layer (the so-called diffuse layer). Ions in the diffuse layer are loosely associated with the surface. The concentration of counter-ions falls off exponentially with increasing distance from the surface and it becomes zero far away where electro-neutrality condition holds. The characteristic length of this exponential decay is called the Debye length ( $1/\kappa$ ), where  $\kappa$  increases as the square root of the ion concentration. When two charged surfaces get close enough that the separation distance becomes of order  $1/\kappa$ , the concentration of counter-ions in the gap becomes higher than that in the bulk. This will increase the osmotic pressure in the gap, which acts to drive the two surfaces apart. This is the root of the electric double layer (EDL) repulsion.

The electric repulsive force increases with surface potential and decreases with higher electrolyte concentration. In turn, surface potential depends on the acidic or basic strengths of the surface groups and on the pH of the solution. The surface charge can be reduced to zero at the point of zero charge (PZC) by suppressing the surface ionization. This can be achieved by decreasing the pH for the case of a basic surface.

The electric double layer repulsion plays important roles in systems that involve aqueous or polar media and it is the basis of the well-known DLVO theory that follows.

### 2.6.5 DLVO theory

Based on the DLVO theory [31], the interaction energy between two colloidal particles could be due to one of the following:

- a) A repulsive interaction  $V_R$  owing to overlap of the electrical double layers. It helps to keep the particles dispersed in solution.
- b) An attractive interaction  $V_A$  owing to van der Waals forces. It acts to destabilize the dispersion through aggregation.

The total interaction energy  $V_T$  is simply the sum of these two energies, i.e.

$$V_T = V_R + V_A \quad (2-12)$$

The final condition depends on the balance between electric double layer repulsion and van der Waals attraction, and it determines the stability of colloidal system in aqueous environments.

Parts of our study were conducted in hydrocarbon (a non-polar environment). Due to very low ions solubility in non-polar liquids, the diffuse double layer will not form in hydrocarbons. Other forces, such as van der Waals attraction, remain important in non-aqueous media.

### 2.6.6 Inter-particle forces in non-aqueous media

In non-aqueous media, the colloidal forces are different from aqueous media. Steric repulsion and cross bridging are two important forces that act along with van der Waals attraction in non-aqueous media.

### 2.6.7 Steric repulsion

Some of colloidal dispersions are stabilized by the adsorption of large molecules or species (e.g. polymers, surfactants, submicron solids) onto the colloidal particle surfaces; this stabilization is caused by an interaction called the steric repulsive force [32]. In our case, bitumen consists of fairly large and heavy molecules. Adsorption of some fractions of these large molecules onto the surfaces of suspended solids can significantly affect particle-particle interactions. For instance, in “good solvents,” large molecules that adsorb onto the surfaces of particles can form a brush-like structure by extending into the solvent. When two particles with covered surfaces approach one another, it will cause the brushes to repel one another, thus leading to a short-range steric repulsion between the particles. In contrast, in “poor solvents,” the molecular brushes will collapse onto the surfaces of particles, thus making it possible for van der Waals attraction to overcome the steric barriers and result in aggregation.

The solvency of the medium and the thickness of the adsorbed layer relative to the particle size are two factors that determine the degree of stabilization.

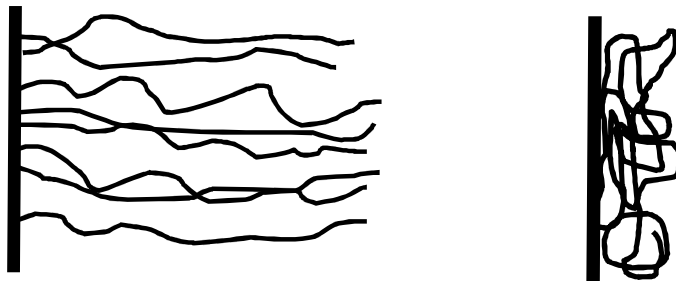


Figure 2.3 large molecules adsorption on the surface in  
a) good solvent (brush like structure) b) bad solvent (packed structure)

### 2.6.8 Cross bridging

Sometimes in colloidal suspensions, the existence of polymers or large molecules can promote aggregation and precipitation of colloids. This occurs when the adsorbed polymers are insufficient to fully cover the particle surface but long and flexible enough to bridge between two particles (when separations are comparable to the size of the polymer); this can therefore provide a link between two neighbouring particles. This is the called “polymer-bridging” flocculation in which polymers can function as flocculants and help to precipitate colloids [33].

In this study, we have not planned to use polymers as an additive and hence the influence of polymer bridging on aggregation will not be studied.

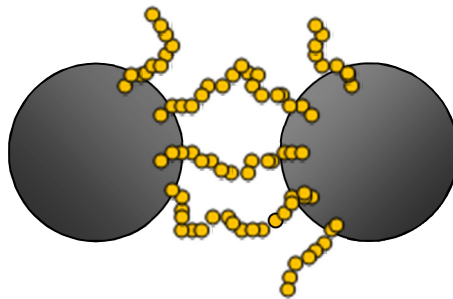


Figure 2.4 Polymer cross bridging between two particles

## 2.7 Particles size measurements method

The size of particles can be determined by Mastersizer (Malvern 3000). This device uses the technique of laser diffraction to measure particle size distributions from  $0.01\mu\text{m}$  up to  $3.5\text{mm}$ . In laser diffraction measurement, a laser beam passes through a dispersed particulate sample and the angular variation in intensity of the

scattered light is measured on a series of detector elements positioned at different angles. Large particles scatter light at small angles relative to the laser beam and small particles scatter light at large angles. The angular scattering intensity data is then analyzed to calculate the size of the particles that created the scattering pattern using the Mie theory of light scattering. The particle size is reported as a volume equivalent sphere diameter.

Obtaining good results from a laser diffraction measurement also depends on setting appropriate measurement conditions such as obscuration range, measurement duration, and stir speed. For instance, a low to medium particulate concentration during measurement is required for good operation. When the particle concentration is too low, the scattered light signals are weak, which cause a low signal-to-noise ratio and poor repeatability. At too high concentrations, a photon scattered from one particle has high probability of being scattered again at one or more other particles (multiple scattering). The concentration limits are usually indicated in terms of obscuration, which is the percentage of incident light that is removed by the particles.

The appropriate sample concentration for a laser diffraction measurement is a balance between adding enough sample to get a sufficient signal to noise, and not adding too many particles so that the measurement is affected by multiple scattering. The sample concentration in a laser diffraction system is measured by a parameter called obscuration, the percentage loss of laser light through the sample.

There is a certain amount of noise in any measuring system. In the Mastersizer, one can see this as small but random fluctuations in the data after the background signal has been subtracted out. If the concentration of particles in the cell is too high, there is a higher probability that the laser light has been scattered by more than one particle before hitting the detector.

## **2.8 Settling rate measurement methods**

Sedimentation measurements permit the investigation of the sedimentation rate of suspensions. There are numerous techniques to measure the initial settling rate of solids.

### **2.8.1 Optical methods**

In optical method, the interface position is tracked during settling by visual observation or particles are made to pass through a focused light beam (usually a laser beam). Then, the transmitted light or scattered light intensity is measured. Each particle passing through the beam causes a reduction in transmitted light or an increase in scattered light. Most of the common light-absorption or light-scattering techniques cannot be used in opaque solutions (e.g. crude oil). Application of this method is only limited to solutions which are sufficiently transparent. If the visibility is low, the motion of the interface cannot be followed easily, and the method becomes ineffective.

Another important consideration is that optical method only works well if the interface between the clear liquid and the dispersed solids remains sharp

throughout. In practice, this interface often becomes more dispersed (i.e. blurred) as settling progresses.

For the present research, we encounter both problems: the suspending liquid (diluted bitumen) can be very opaque, and the interface between the supernatant and solids suspension tends to become very diffuse.

### **2.8.2 Ashing technique**

In very dark suspending liquids, light cannot pass through the medium. Therefore, methods which are based on light detection are not applicable. Ashing technique is an alternative method to measure the settling rate in dark liquids. In this method, the solids concentration changes are monitored by extracting samples from a sedimenting suspension at fixed depths and predetermined times. The advantage is that the instrumentation is relatively cheap. In this method, each withdrawn sample is analyzed for solids content by burning away all aqueous and organic contents, leaving behind only the inorganic ash. A plot of the mass  $m$  of the residual solids (at a fixed location) versus time can provide useful information on the sedimentation process. The slope of the initial part of the  $m$  vs  $t$  plot can be used as a representative measure of the settling rate (Figure 2.5).

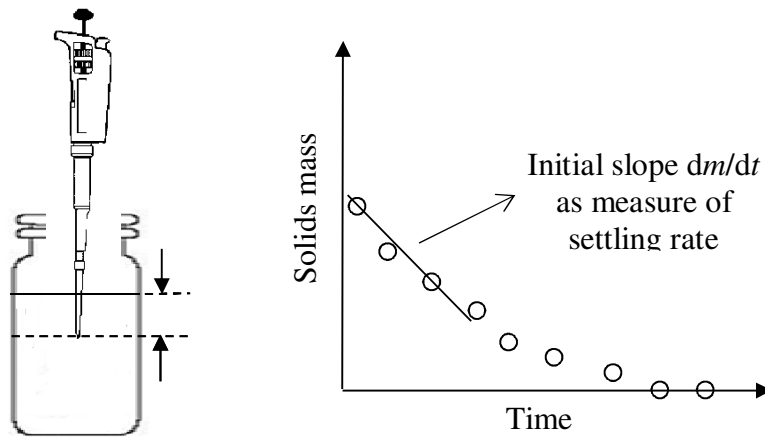


Figure 2.5 (a) Schematic of the settling experiment. Samples were taken from a fixed location 1 cm from the free surface. (b) Typical plot of solids content in the sample versus time[17].

A drawback of this manual technique (fixed or variable pipette techniques) is that they are fairly labour intensive, time consuming (up till 8 hrs for small particle sizes) and sensitive to operator skills.

In this study, we introduced a new method of quantifying settling rate of particles by tracking the solids content at a fixed location over time using a sedimentation balance (KRÜSS K100).

### 2.8.3 Sedimentation balance

In sedimentation balances, the suspension is allowed to settle in a temperature-controlled environment while the weight of sediment is measured as it accumulates on a measuring probe.

The measuring body is suspended from the force sensor and collects the deposited particles at a fixed location below the liquid free surface.

A built-in magnetic stirrer also provides a homogeneous suspension until just before the measurement is made. When the stirrer is switched off the suspended particles begin to sink to the bottom. The measuring probe catches the sinking particles and records their weight as a function of time; this allows the sedimentation rate to be determined. One of the advantages of this method is that it gives a continuous record and is capable of analysing samples weighing as little as 0.01 mg.

In literature, some other methods were also successfully used to follow the settling of particles in opaque liquids. They are discussed as follows.

#### **2.8.4 X-ray method for detection of the settling solids**

Ondeyka [34] developed an indirect X-ray technique to follow the settling of mineral particles in opaque liquids such as coal-derived liquids at high temperatures and pressures. In this technique, the interface was photographed at certain time intervals during settling and settling curves and settling rates were then deduced from the X-ray images. The fact that the mineral particles attenuate X-rays to a much greater extent than the liquid is the basis of this method. It is worth mentioning that sampling in direct methods disrupts the settling phenomena to some extent. In contrast, the indirect X-ray method produces photographs showing the solids settling front without disturbing the sedimentation processes. The X-ray methods are limited to materials having a high atomic mass (i.e. X-ray opaque material).

### 2.8.5 In line monitoring methods

Long and Dabros [34] successfully used an in-line transfectance probe to monitor the settling of WD/DS/PA aggregates in solvent-diluted bitumen. The probe is coupled with a near infrared (NIR) spectrophotometer via a fiber-optic cable. Figure 2.6 illustrates the experimental setup.

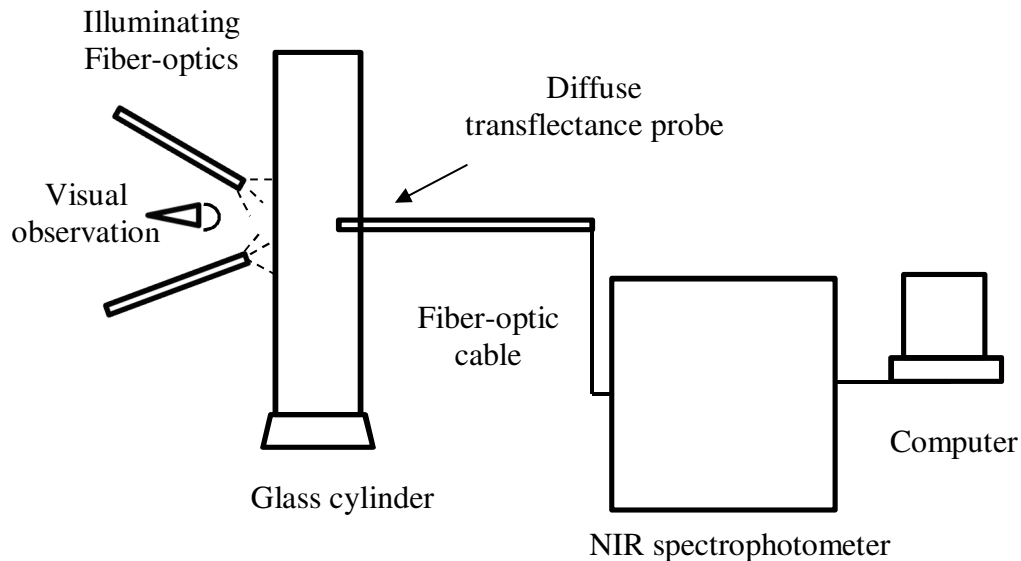


Figure 2.6 In-line experimental setup

A specially designed diffuse transfectance probe is inserted horizontally through a side opening in the settler and is, therefore, immersed in the solvent diluted bitumen emulsion, thus providing direct in-line monitoring of the settling process. Incident monochromatic light is partially scattered and absorbed by the solution and the WD/DS/PA aggregates. The scattered light is detected by the in-line probe. The signal returning to the spectrophotometer thus contains information that reflects the instantaneous local composition of the solvent-diluted bitumen emulsion.

## 3 Material and method

We would like to investigate the aggregation behavior of silica particles in water and solvents (similar to what occurs in paraffinic froth treatment). This chapter discusses the details regarding sedimentation experiments.

### 3.1 Solvents

For these experiments, toluene and *n*-heptane, both HPLC grade, were purchased from Fisher Scientific and used as received. Also, ultra-pure water (resistivity $\approx$ 18.2 M $\Omega$  cm) was freshly collected from a Millipore Milli-Q system.

### 3.2 Silica particles

Experiments were performed using one type of solids. Spherical silica particles with diameter of approximately 1  $\mu$ m were purchased from Fiber Optic Center (Massachusetts, USA). The silica particle density is approximately 2100 kg/m<sup>3</sup>. In this study, 1  $\mu$ m silica particles were surface modified in two different ways, resulting in what we will call “clean” and “bitumen-coated” particles.

#### 3.2.1 Clean silica

To prepare clean silica particles for our experiments, the factory received particles were heated in a muffle furnace (Thermo-scientific Thermolyne heavy duty muffle furnace, model FA1730) at 650°C for 2 hours to remove any possible chemical residue on the surface. Then, the clean particles were used for experiments.

### 3.2.2 Bitumen-coated silica

In this study, 1  $\mu\text{m}$  silica particles were surface modified by coating a layer irreversibly adsorbed bitumen material onto the particle surfaces. The bitumen used for coating was the so-called ‘vacuum topped’ sample provided by Syncrude Canada Ltd. The toluene was HPLC grade from Fisher Scientific and was used as received without further purification.

### 3.3 Preparation of bitumen coated silica

The method we used for surface coating is as follows: To begin, a toluene-diluted bitumen solution at 1:4 wt. % ratios were prepared. Then clean silica particles were dispersed in toluene-diluted bitumen at 5 wt. % (e.g. 5 g of clean silica in 100 g of diluted bitumen solution). To ensure that all the silica particles were completely wetted and no dry mass remained in the suspension, 15 mL of toluene was first added to the silica powder to make them wet. After 2 minutes of mixing, the diluted bitumen solution was added. Teflon bottles (NALGENE Labware, FEP material) were used for all preparation steps to minimize the attachment of silica particles to the container walls. Next, the suspension was mixed by a magnetic stirrer for 24 hours to allow adsorption of bituminous material onto the silica particle surfaces. Following this, the silica particles were washed with fresh toluene and centrifuged using a centrifuge (Beckman, model JA-10).

In the washing procedures, the bitumen-coated particles were centrifuged for 15 minutes at 4000 rpm until the supernatant was free of solids. The supernatant was then discarded and replaced with another 30 mL of clean toluene. The suspension

was vigorously agitated, then centrifuged again. The washing process was repeated several times until the supernatant became colorless. The colorless solvent means that the remaining deposited bitumen on the surface has strong bonding with the silica surface and it could not be washed away with toluene. As a result, organics which remained on the particle surfaces are considered irreversibly adsorbed. Next, the slightly blackened powder, which was our bitumen-coated silica particles, were dried under a fume hood for 2 days. It is assumed that the silica particles that have undergone this special type of surface modification are similar to the particles that have been in contact with bitumen for extended periods of time in oil sand ores.

### **3.4 Sample preparation for settling tests**

To study the settling behavior of bitumen-treated silica particles in hydrocarbon environments, solvents consisting of different volume ratios of heptane to toluene, namely heptol mixtures, were used in our experiments. Heptol solutions were specified by their toluene content in volume percentage; it ranged from 0% (i.e. pure *n*-heptane) to 100% (i.e. pure toluene). To extend our studies to more realistic oil phases, de-asphalted bitumen or full bitumen were added to the heptol solution. The amount of oil in the heptol solution varies from 0 wt% (i.e. only heptol) to 3 wt% de-asphalted bitumen; 4.5wt% full bitumen was also used in some experiments. Prior to experiments, 1- $\mu\text{m}$  spherical silica particles (Fiber Optic Center Inc) have been pre-exposed to bitumen to change the surface properties of silica particles through adsorption of bituminous material.

After preparation of the hydrocarbon solution, 5 wt% of silica particles were added to 50 g of solvent in a bottle. The solution was then agitated in a water bath sonicator (Fisher Scientific, model FS30) for 15 minute to create a homogenous suspension. Following this, 3 wt% of oil was added to the solution. To prevent attachment of particles to the container walls, Teflon bottles were used for these experiments. Figure 3.1 shows the sample preparation procedures.

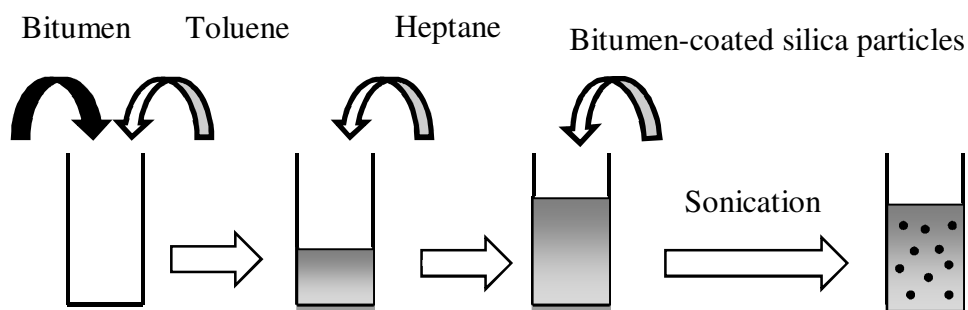


Figure 3.1 Sample preparation procedure in a Teflon bottle

### 3.5 Preparation of de-asphalted bitumen

Bitumen can be dissolved in aromatic solvents. However, when bitumen is mixed with an alkane solvent, such as heptane, it is divided roughly into 2 components: asphaltenes and maltenes. Asphaltene is the part that is not soluble in an aliphatic solvent and it contains the highest molecular weight components of bitumen. Maltene is the part that is soluble in an aliphatic solvent and it consists of moderate to low molecular weight components: resins, aromatics and saturates. The amount of precipitated asphaltene depends on the solvent-to-bitumen ratio and on the carbon number of the alkane solvent being used.

In part of our study, the diluted maltene (de-asphalted bitumen) was used as the continuous phase; the solvent precipitation method was used to produce de-

asphalted bitumen. The procedures are as follows: Heptane was first mixed with bitumen at a ratio of 40:1 by volume. The mixture was agitated by a magnetic stirrer for 2 hours and then left for 24 hours to allow the asphaltenes to precipitate out from solution. A 0.22- $\mu\text{m}$  vacuum filter (Fisher Scientific, 47 mm all-glass vacuum filter holder) was used to separate the precipitated asphaltenes from the aged mixture. The added *n*-heptane was then removed using a rotary evaporator. To remove the remaining asphaltenes in the bitumen, this process was repeated at a 4:1 ratio by volume (4 parts *n*-heptane + 1 part bitumen). The separated asphaltenes were washed multiple times with fresh heptane and left under a fume hood to dry by naturally evaporating the heptane solvent. Then, the total asphaltene weight was obtained. Calculation showed that the asphaltene content was about 35% of the original bitumen.

### 3.6 Settling rate measurement

In this study, we introduced a new method of quantifying the settling rate of particles by tracking the solids content at a fixed location over time using a *sedimentation balance* (KRÜSS K100). This device consists of a measuring probe that collects sediments and is connected to a sensitive balance. The probe location is fixed at a distance below the liquid surface. A sketch of the experimental setup is shown in Figure 3.2.

The particle settling rate can be an indicator of how fast the fine solids can form aggregate clusters and settle to the bottom of the test bottle. The objective here was to understand the relation between the solids settling rate and the type of hydrocarbon solvent that was used.

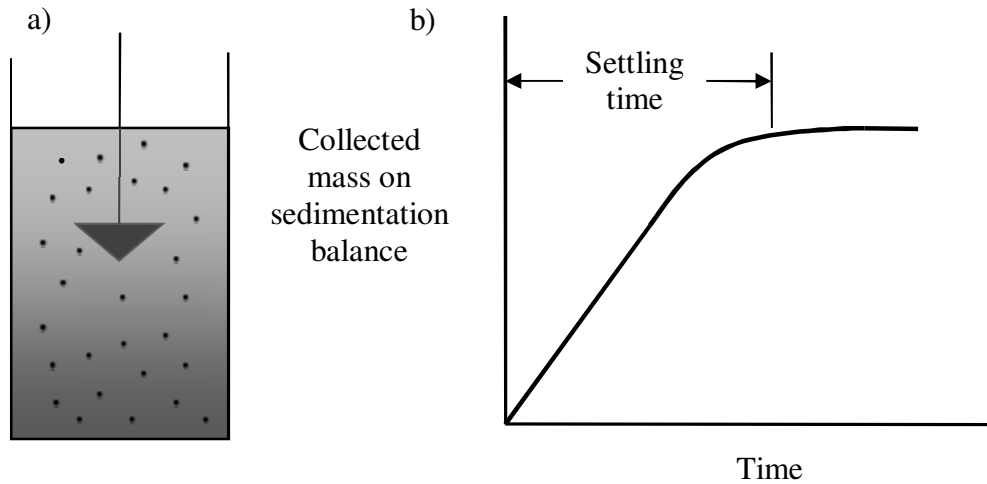


Figure 3.2 A schematic of sedimentation experimental set up, b) a typical plot of the solids mass  $m$  vs. time  $t$  in settling experiments

As discussed in Chapter 2, this is a more suitable approach than the common method of following the zone interface (i.e. the interface between the top clear liquid and the “mud”). The traditional method, which is based on optical detection of the sludge zone interface, was not applicable here because of the opacity of the solution whenever bitumen was present in the system. Our new method of quantifying settling rates proceeded as follows: As mentioned above, a suspension of evenly dispersed particles in hydrocarbon was prepared by adding silica particles to the suspending liquid and applying 5 minutes of sonication. As the particles aggregate and settle, the solids content on the probe would increase over time. The weight change of the probe is an accurate measure of the solid content ( $m$ ) as time ( $t$ ) passed.

A typical plot of the solids mass vs. time is shown in Figure 3.2b. The starting time was defined as the moment when the built-in stirrer stopped and the solids were allowed to settle under gravity. The time that the mass on the probe reaches

a constant value is taken as a measure of the solids settling time. In this study, we define the normalized settling rate as the collected mass on the probe at any time divided by the total mass collected over infinite time (i.e.  $\frac{dm}{dt} \times \frac{1}{\Delta m}$  ). This parameter represents the slope of the fractional mass vs time plot (units of inverse second), which is independent of the density of settling particles.

## 4 Results and discussion

We wish to study the sedimentation of fine solids (i.e. 1- $\mu\text{m}$  silica particles) suspended in water and hydrocarbon media. To begin, the particles sizes were measured by mastersizer 3000 (Malvern); the solid particles were then surface-modified following the procedure described in Section 3.

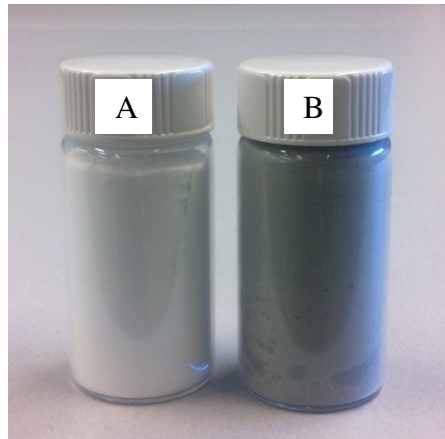


Figure 4.1 A) Clean silica particles B) Bitumen-coated silica particles

Next, the hydrocarbon phase was prepared and the silica particles were dispersed in the hydrocarbon by sonication. The sedimentation behaviours of first silica particles in water, then surface modified silica particle in hydrocarbon (i.e. heptane-toluene mixture), were studied. The independent variable for water was the pH; in the hydrocarbon medium, the independent variable was the aromatic (i.e. toluene) content in heptol. In both cases, the dependent variable was the settling rate, which was taken to be the collected mass on the probe at any time divided by the total mass collected over infinite time (i.e.  $\frac{dm}{dt} \times \frac{1}{\Delta m}$ ). This parameter is an indication of mass fraction over time (units of inverse second), which is independent of the density of settling particles. The reason for the differences in settling rates can be traced to the inter-particle forces. As discussed

in Chapter 2, there are several factors that profoundly affect both the forces and the sedimentation rate. These factors include the solid material (and any surface modification that the particles have been subjected to) and the properties of the surrounding media. In this study, we began our experiments with water and pure solvents, and developed the work by adding 3 wt% de-asphalted bitumen and 4.5 wt% bitumen to the heptol mixture. Adding de-asphalted bitumen and full bitumen to the suspending medium provides a better simulation of the solvent-based extraction process, as explained in Chapter 1. Furthermore, we could investigate the effect of bitumen components on particle sedimentation at fixed solids content of 5 wt%.

The various systems that were studied using sedimentation balance are listed below in Table 4.1.

Table 4.1 Solids and the corresponding hydrocarbon phases that were studied.

Solids (silica) particles	Suspending liquid
Clean silica	Water
Clean silica	Toluene
Bitumen coated silica	Toluene
Bitumen coated silica	Heptol (pure solvent)
Bitumen coated silica	Heptol diluted maltenes
Bitumen coated silica	Heptane diluted bitumen

## 4.1 Particle size distribution measurement:

It has been reported that problematic solids in real froth are ultrafine solids of size less than 10  $\mu\text{m}$ . In this study, we used silica as the model solid in the settling experiment. In order to determine the particle size distribution (psd), the Mastersizer 3000 (Malvern) was used. Figures 4.2 and 4.3 show the particle size distributions of clean and treated silica beads.

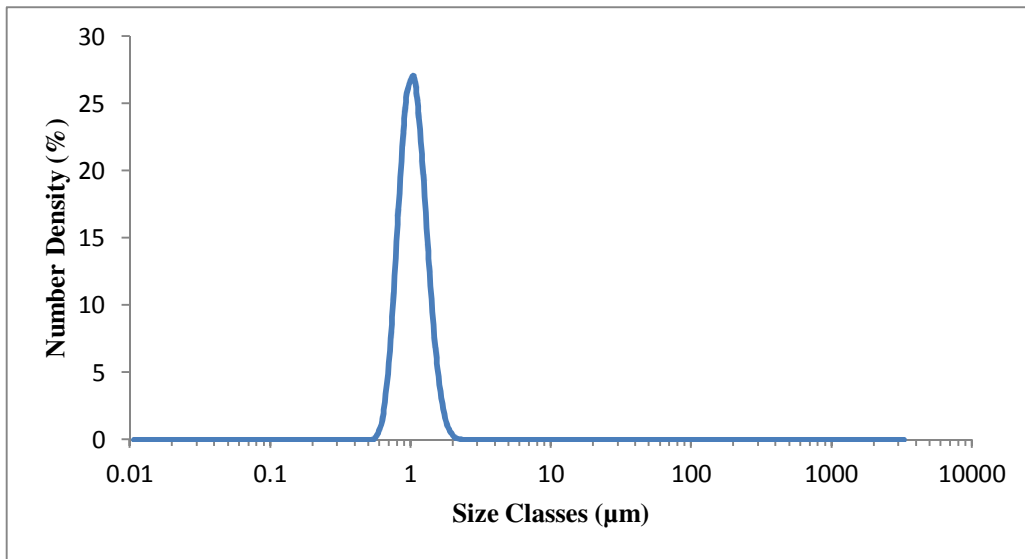


Figure 4.2 Particle size distribution of clean silica particles in water

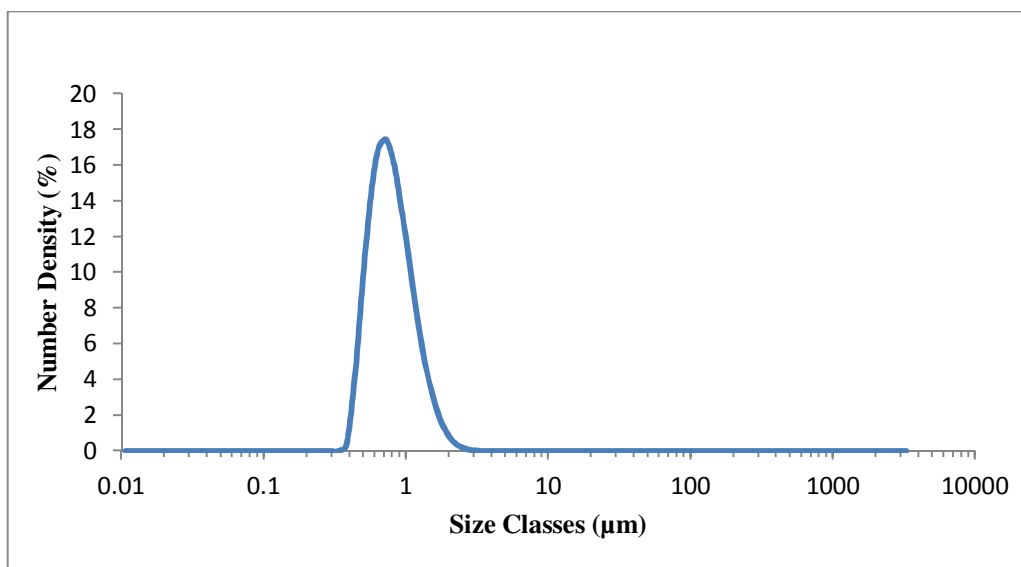


Figure 4.3 Particle size distribution of treated silica particles in toluene

The  $d_{50}$  is defined as the size where half of the population has the value below this diameter on the number distribution diagram; it is also called the median of the particle size distribution. The  $d_{50}$  for clean and treated silica beads are shown in Table 4.2.

Table 4.2 Median particle size of samples used in the experiments.

Samples	$D_{10}$ ( $\mu\text{m}$ )	$D_{50}$ ( $\mu\text{m}$ )	$D_{90}$ ( $\mu\text{m}$ )
Treated silica beads (in toluene)	0.518	0.760	1.25
Clean silica beads (in water)	0.787	1.03	1.37

The results show, as expected, treatment of particles did not change the particles size distribution.

## 4.2 Sedimentation in water:

To begin our study at a preliminary level, particle sedimentation tests of clean silica in water were first studied at different pH values. The water used in this experiment was Milli-Q water without any ions. As described in Chapter 2, all surfaces bear an electric charge when immersed in an aqueous environment, consequently the double layer forms. The magnitude of surface charge and the thickness of the double layer can be manipulated by the pH. According to DLVO theory, the balance between electric double layer repulsion and the van der Waals attraction determines the stability of colloidal system in aqueous environments.

The results, as plotted in Figure 4.4, show collected mass from sedimentation of clean silica particles vs. time in water with different pH values.

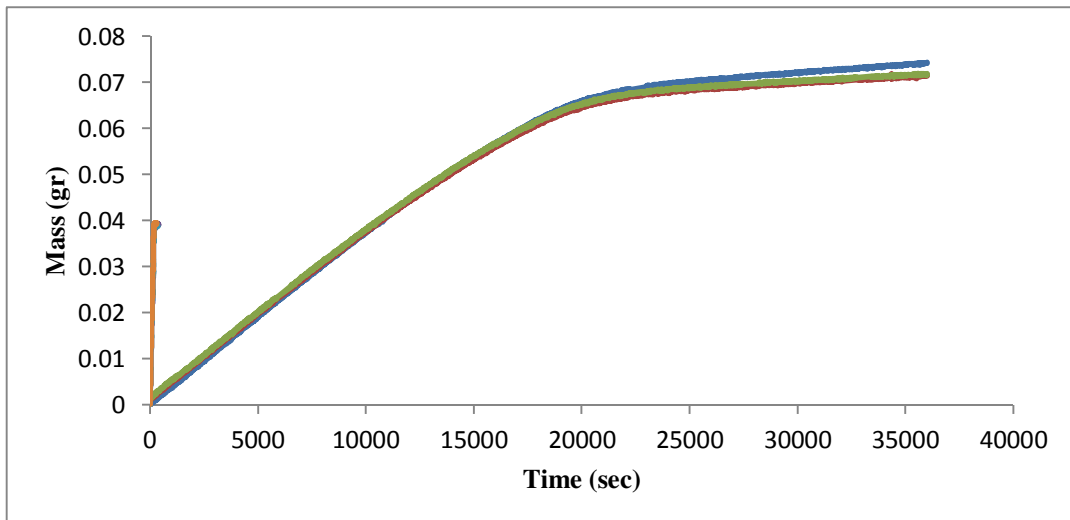


Figure 4.4 Sedimentation behavior of clean silica particles in water with pH 6.8 and pH 2

For particles carrying similar surface charges, the electric force is repulsive.

The value of pH was used to describe point of zero charge for systems in which  $H^+/OH^-$  are the potential-determining ions. When the pH is equal to 2, the surface of silica beads bear zero charges; consequently, the double layers vanish, and the repulsive force between the silica beads disappears and the attractive force (van der Waals) become effective and particles tend to aggregate rapidly.

Conversely at higher pH (such as pH 6.8), the particles carry a negative charge, thus giving rise to double layers formation. The two solid spheres experience an increasing repulsive force as they approach each other, and destabilization (i.e. aggregation) is prevented.

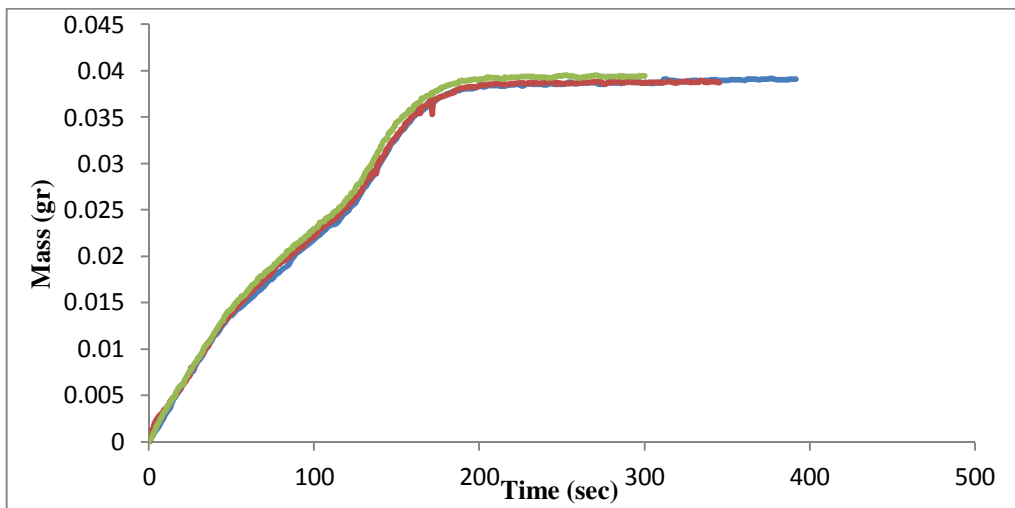


Figure 4.5 Sedimentation behavior of clean silica particles in water with pH 2

### 4.3 Sedimentation in organic solvents:

In this section, we investigate the settling behaviour of clean particles and treated particles in toluene. The results are presented in Figure 4.6. In this figure, the horizontal axis represents the time in second, and the vertical axis is the collected sediment in milligrams. For clean silica beads, the settling time was less than a

minute; in sharp contrast, for treated particles, it was 3.5 hours. As the clean beads settled much faster than bitumen-treated beads, it is reasonable to infer that the aggregate sizes were bigger in the case of clean silica. The reason behind this is that when clean silica particles are immersed in an organic solvent, the double layer will not form due to very low ion solubility in non-polar (hydrocarbon) liquids. Thus, the particles can collide and easily attach to one another via van der Waals attraction.

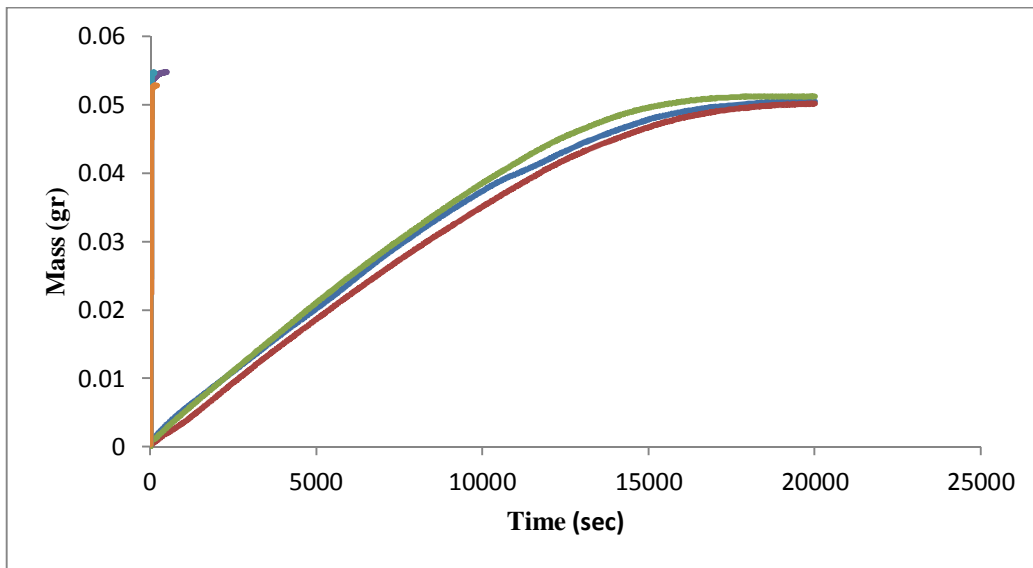


Figure 4.6 Sedimentation behavior of clean silica and treated silica particles in pure toluene

In the case of treated particles, the much lower settling rates can be interpreted as increased colloidal stability. This stability is due to the presence of polymer-like chains on the surfaces of the silica particles. The polymer acts as hairy materials that prevent particles from approaching one another.

Continuing further, we postulate that the particle-particle attraction between clean silica beads must be stronger than that among bitumen-coated particles due to the

presence of steric barrier among bitumen-coated particles. Also, if strong repulsion exists between the particles, the collision efficiency will be very low and aggregation will occur only very slowly.

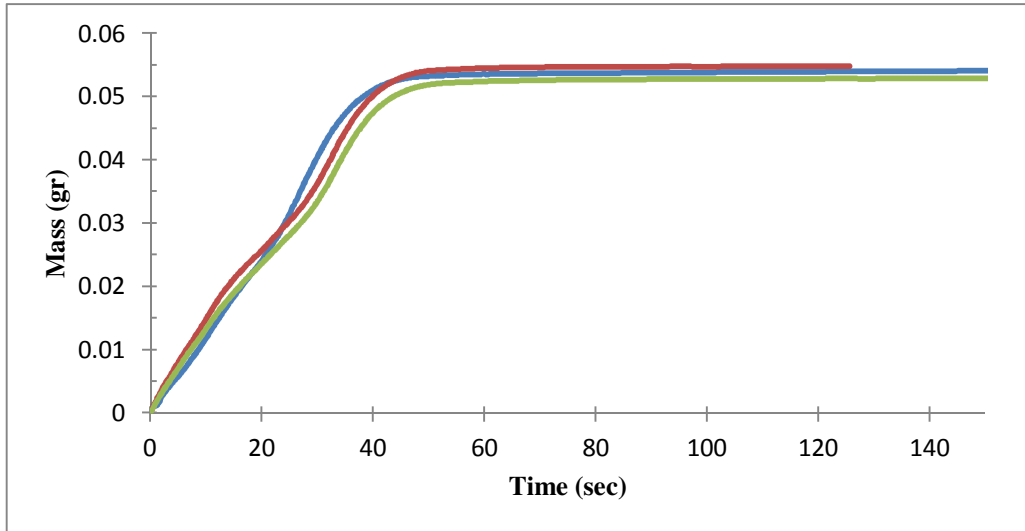


Figure 4.7 Sedimentation behavior of clean silica particles in pure toluene

#### 4.4 Effect of oil phase composition on solids settling rate

The ultimate objective here is to understand the settling behavior of fine solids in diluted bitumen. As discussed in Chapter 1, it is related to the removal of unwanted solids in a non-aqueous bitumen extraction process. In this study, the factors that were kept constant throughout all experiments were: the type and size of the primary particles (1  $\mu\text{m}$  silica spheres), the method through which the particles were surface-modified (exposure to toluene-diluted bitumen), and the solids content (5 wt%). As such, changes in sedimentation rates can result only from changes in the composition of the suspending liquid. The suspending liquid,

which is the oil phase, can be heptol, heptol + de-asphalted bitumen, or heptol + full bitumen.

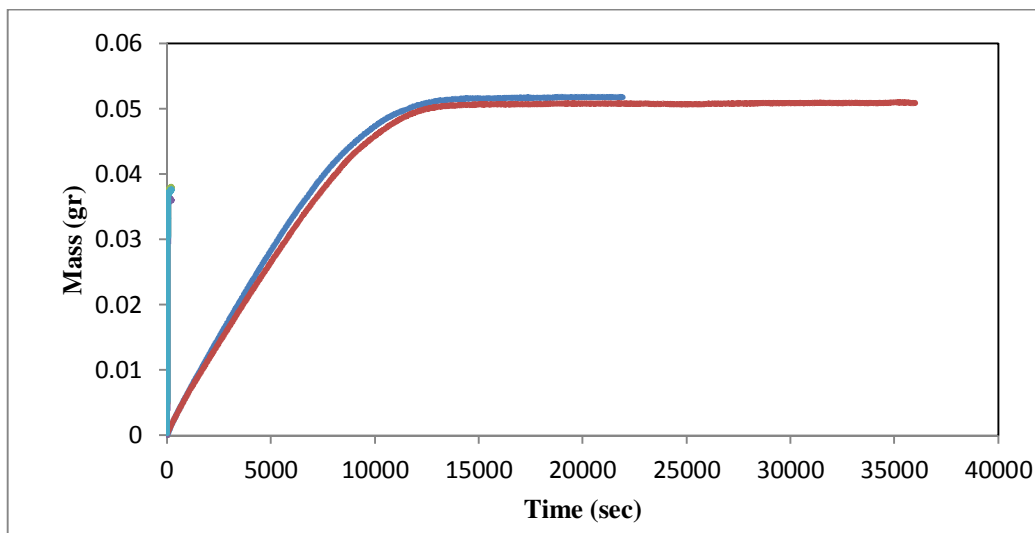


Figure 4.8 Sedimentation behavior of treated silica in toluene and heptane + 3% de-asphalted bitumen

In this section, we performed the settling experiment with treated silica particles in toluene and heptane. The results, as plotted in Figure 4.8, show the times that treated silica particles take to travel a 15-mm distance in a toluene-rich mixture; this time duration is on the order of hours. However, in the case of a paraffinic mixture (here, heptane), the duration is on the order of seconds. We speculate that, for solvents containing significant amounts of aromatic components (here, toluene), the silica particles will repel one another at close range. The reason must be due to surface modification of the silica particles by bitumen: one may speculate that the higher molecular weight components of bitumen (asphaltene molecules) will be attached to the silica particle surface, forming an irreversibly adsorbed layer.

Table 4.3 Calculated settling time and observed settling time in different hydrocarbon used in the experiment.

Solvent	Calculated settling time base on Stokes' law	Observed settling time
Toluene	3.66 hr.	3.56 hr.
Heptane	2.2 hr.	50 sec

As discussed in Chapter 2, these large molecules will extend into an aromatic environment (owing to its high solvency), forming a “swollen brush” around the particle. As shown in Figure 9a, when two particles with asphaltene-coated surfaces approach one another, the adsorbed layers behave as steric barriers and result in a repulsive force. This steric repulsion is responsible for the overall colloidal stability of the particles in toluene, and therefore according to Stokes law, a very slow settling velocity (of order  $1 * 10^{-6}$  m/s) is expected in solvents with high aromatic contents.

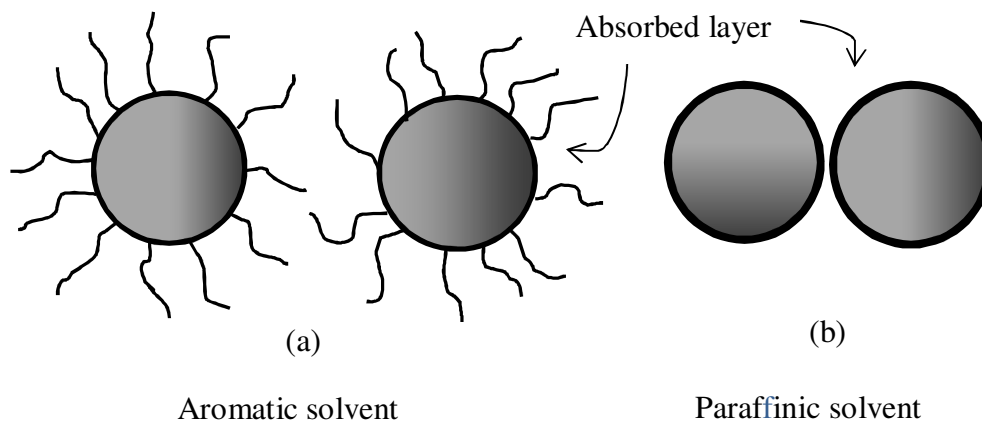


Figure 4.9 Bitumen-coated solid particles in (a) a paraffinic solvent, (b) an aromatic solvent

On the other hand, by replacing the aromatic solvent with a paraffinic one (e.g. *n*-heptane, which is a “bad solvent” for asphaltene molecules), the molecular brushes (shown in Figure 4.9b) will get smaller or collapse onto the surfaces. With the collapse of the steric barriers, the particles are allowed to get sufficiently close to one another for van der Waals attraction to be effective. As a result, aggregates will be formed that finally grow to sizes which settle rapidly. Thus, one could see that higher paraffinic contents of the organic solvent could result in bigger aggregates, which in turn leads to faster settling rates.

In addition, calculated settling times based on Stokes law and observed settling times in experiments for pure solvents are shown in Table 4.3. In the case of toluene, the calculated Stokes time is similar to the observed settling time. Here, we relate this similarity to well-dispersed and non-aggregating treated silica particles, which move downward under gravity at the rate of an isolated single particle. On the other hand, the observed rapid settling rate in heptane could be a consequence of broad particle size distribution as a result of significant aggregation of the 1-micron silica particles.

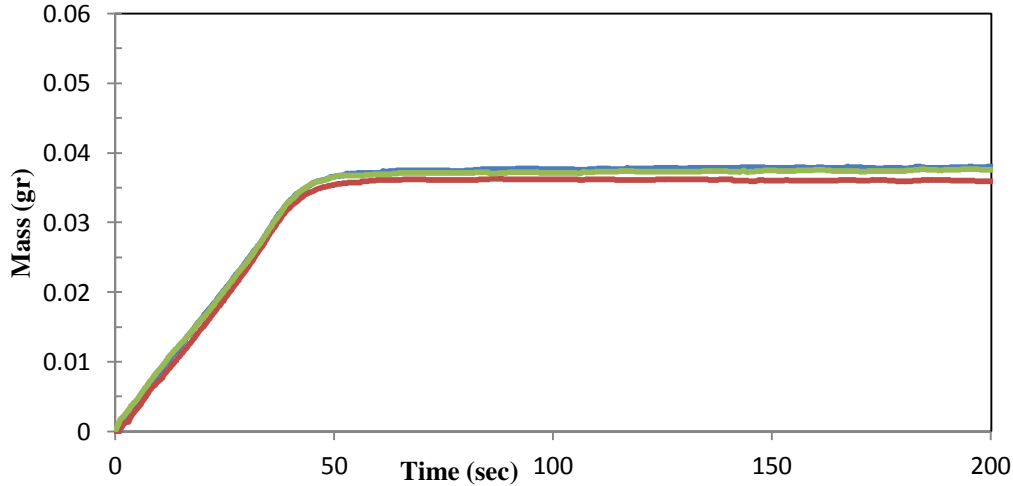


Figure 4.10 Sedimentation behavior of treated silica in heptane + 3% de-asphalted

## 4.5 Settling rate

In this set of experiments, the oil phases consist of a mixture of *n*-heptane and toluene (i.e. heptol) at different volume ratios. The different ratios of toluene-to-heptane in the solvent medium is a tactic to alter the aromatic content of the surrounding medium; it varies from 0 vol% toluene (i.e. pure *n*-heptane) to 100 vol% (i.e. pure toluene). As discussed in Chapter 2, the continuous medium's aromatic content in suspension can influence the inter-particle forces and thus the sedimentation rate.

Sedimentation experiments of bitumen-coated silica were initially conducted in pure heptol (i.e. 0 wt% bitumen). The results are shown in Figure 4.11. In this graph, the horizontal axis represents the amount of toluene (in volume percentage) in the heptol mixture; this can be interpreted as the degree of solvent aromatic content. The vertical axis is the normalized settling rate of the solid particles. Each data point in Figure 4.11 shows the settling rate of solid particles in different

organic solvents (i.e. different aromatic contents in the heptol mixture). Each data point is the average settling rate of at least 3 measurements.

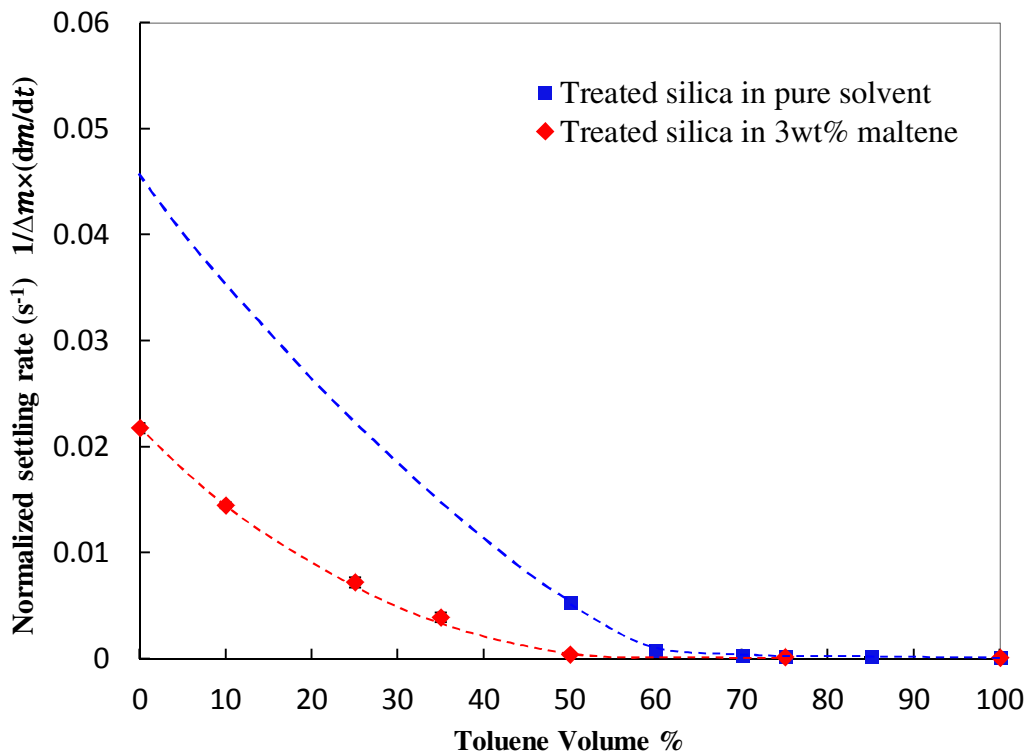


Figure 4.11 Effect of addition of 3 wt. % maltene on the settling rate of bitumen-treated silica in heptol (a mixture of toluene and n-heptane). The dotted blue line is the expected settling rates below 50 vol. % toluene content in heptol.

The results show that the settling rate of bitumen-coated silica depended strongly on the aromatic content of the solvent: the higher the aromatic content (i.e. higher toluene ratio), the lower the settling rate. Lower settling rates can be interpreted as increased colloidal stability. We were not able to perform experiments for toluene content less than 50 vol% due to the high affinity of the particles to each other and also to the shaft of the balance (particles stuck to the shaft of the balance will contribute to a significant amount of added mass that is unrelated to

sedimentation). The expected settling rates below 50 vol% toluene have been extrapolated.

In the next step, the simple case of bitumen-treated silica settling in heptol was modified to a more realistic situation: the new oil phase is now heptol-diluted maltene (the same solid particles, i.e. bitumen-treated silica, were used). The solids concentration was kept constant at 5 wt%, and the bitumen concentration was 3 wt%.

The effect of bitumen concentration on the settling rate is also shown in Figure 4.11. In the presence of maltene, the settling rates of silica particles show the same dependency on the aromatic content of the solution (compared to cases of pure solvent, i.e. in the absence of maltene). Interestingly, addition of maltene to the system leads to overall decrease in settling rates.

As shown in Figure 4.11, in pure solvent, the settling rates in toluene content more than 70 vol% are very low (order of  $10^{-4} \text{ s}^{-1}$ ) and effectively zero. However, with addition of maltene to the system, the settling rates are effectively zero for toluene content of more than 50 vol%. The observed non-zero settling rates at low toluene contents could be a consequence of significant aggregation of the silica particles. In addition to this, earlier studies in our group [17] had demonstrated that the settling behaviour of bitumen-coated silica particles in heptol (as an organic solvent) strongly correlated with the nature of the inter-particle forces. Interaction between bitumen-treated surfaces (with main focus on asphaltenes) can be attractive or repulsive, depending on the “quality” of solvent. We speculate that in the toluene-rich end of the settling rate curve (Figure 4.11),

the nature of inter-particle forces is steric. Even though there may still be some attractive force, it seems that in a “good solvent,” repulsive forces are dominant. Due to these repulsive forces, one can conclude that the solids suspension is colloidally stable. As mentioned in Section 2.6, there are different types of adhesive forces between colloidal particles. Most of these forces, however, are not applicable in our non-aqueous environments. We propose that the main attractive forces are due to van der Waals interaction. Depending on the aromatic content of the solvent (which alters the inter-particle separation), the magnitude of the van der Waals forces can significantly change.

According to the above hypothesis, the aromatic content of the solvent has strong effects on the magnitude of the inter-particle forces; this is in agreement with a previous study based on force measurements [17] and also with the sedimentation behaviour presented in Figure 4.11.

As discussed in Chapter 2, the van der Waals force between two identical spheres varies inversely with the square of the separation, i.e.

$$F_{vdW} \sim -\frac{A}{D^2}$$

where  $D$  is the separation distance between two surfaces, and  $A$  is the effective Hamaker constant of the system [33]. Changes of the Hamaker constant is likely negligible with addition of 3 wt% maltene to the system [35]; hence, we speculate that the presence of maltene molecules increases the separation distance  $D$  between two particles and interfere with the van der Waals force. Based on force measurement results in  $n$ -heptane, the separation distance between two bitumen-coated particles increases by 1.38 times when maltene is added to the system.

This analogy explains the general decrease in measured forces after addition of maltene and also the shift in effective zero force from 70 vol% toluene in pure heptol to 50 vol% toluene in the presence of maltene (Figure 4.11).

We already have information on how colloidal silica behave in diluted maltene. As seen in Figures 4.11, when there was very little or no aromatic content in heptol, the silica particles aggregated strongly with one another (i.e. homo-aggregated) and settled rapidly. These experiments, however, were quite artificial as they were carried out in the absence of asphaltene precipitates. A more realistic scenario would be for the silica to settle in heptol diluted bitumen. We wish to understand how the silica particles would aggregate in heptol-diluted bitumen, especially when the solvent is close to pure *n*-heptane (i.e. near 0 vol% toluene). In this regime, the aggregation of fine solids can be due to (a) entrapment of fines by the precipitated asphaltene networks, and/or (b) homo-aggregation of the fines in the surrounding hydrocarbon. As the latter mechanism has not been considered by the research community, it is this matter that we shall focus our attention on.

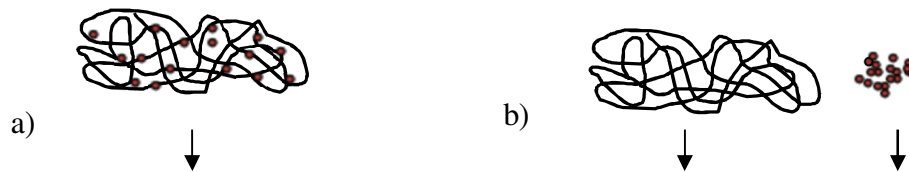


Figure 4.12 Possible mechanisms for paraffinic froth treatment: a) asphaltene network particulate entrapment, b) homo-aggregation of solid

If bitumen were mixed with an aliphatic solvent, its two components will appear as follows:

- The maltenes will be dissolved, forming a solution which we call “diluted maltene.”
- The asphaltenes will first nucleate as small “primary particles” that are distributed throughout the suspending medium (diluted maltene). As these particles collide and adhere to one another, they quickly form loose networks that are more dense than the suspending medium and thus begin to settle. If there is no mechanical agitation in the system, differential settling will be the dominant mechanism of inter-particle collision. Differential settling is a “self-amplifying” effect which can significantly shorten the sedimentation time of colloidal particles, often by orders of magnitude.

The focus of this study, however, is not on asphaltene precipitation; it is on the sedimentation and separation of colloidal silica (or any other type of inorganic solids) in diluted bitumen. For simplicity, we focus only on situations where the diluting solvent is *n*-heptane (i.e. heptol with 0% toluene). In such cases, the settling of inorganic solids would occur concurrently with the precipitation/sedimentation of asphaltenes. The central question is: how will precipitation of asphaltenes affect the homo-aggregation of silica? In the investigation which follows, we will use settling rate (defined in Section 3.6) as an indicator of aggregation and sedimentation. (Due to the opacity of crude oil and the obstruction of asphaltene precipitates, direct microscopic observation is not possible.) Also, for reasons that will be explained later, we will begin our sedimentation balance measurements at a shallow depth of 15 mm.

We begin by comparing the settling rates of (A) silica alone, and (B) asphaltenes alone — both in diluted maltene solutions of the same maltene content. The settling of silica in 3 wt% diluted maltene is shown by Curve A of Figure 4.13; the corresponding settling rate is  $0.022 \text{ s}^{-1}$  (the same rate as shown in Figure 4.11 for 0% toluene).

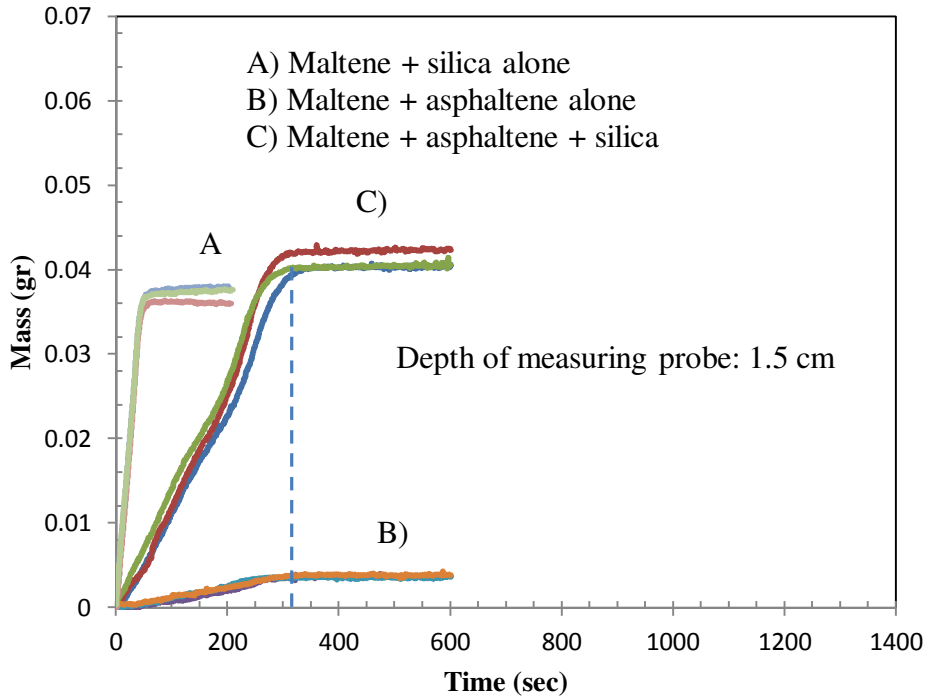


Figure 4.13 The settling curve for Case A) bitumen-coated silica particles in 3 wt. % diluted maltene, Case B) precipitated asphaltenes in 4.5 wt. % diluted bitumen (no silica particle) and Case C) bitumen-coated silica particles in 4.5 wt. % diluted bitumen; collecting tray is located at depth of 15 mm.

Next, the settling of precipitated asphaltenes in 4.5 wt. % diluted bitumen is depicted by Curve B of the same figure. (Reason for choosing such a concentration: 4.5 wt. % diluted bitumen  $\cong$  3 wt% diluted maltene + precipitated asphaltenes.) In this case, the settling rate was  $0.0035 \text{ s}^{-1}$  — roughly seven times slower than that for silica alone. Cases A and B were control tests whose results

are needed for comparative purposes. The next case to be tested, Case C, would address the crucial question of how precipitated asphaltenes affect the homo-aggregation of inorganic solids. This case involved the sedimentation of silica in 4.5 wt% diluted bitumen; this, we reasoned, was equivalent to the settling of silica particles + precipitated asphaltenes, all in 3 wt% diluted maltene. The settling curve for Case C is shown also in Figure 4.13. Interpretations of this curve proceed as follows:

We first note that the steady state mass of Curve C (the plateau value) is the sum of the steady state masses from Curves A and B. This “mass balance” is very significant: it suggests that all silica particles in Case C settled in an “accelerated” manner — either through homo-aggregation amongst themselves, or hetero-aggregation with the asphaltene networks. Free silica particles, with a diameter of 1  $\mu\text{m}$ , would effectively be “neutrally buoyant” on time scales relevant to Figure 4.13; as such, they would not be detected by the sedimentation balance. If any appreciable amount of colloidal silica were free (i.e. not aggregated), we would not have the observed mass balance.

It is seen from Figure 4.13 that the settling rate in Case C was practically the same as that for Case B (involving only asphaltene networks); this is another very important observation: From the apparent mass balance, we had deduced that all silica particles in Case C participated in either homo-aggregation or were captured by the asphaltene networks. Yet, if homo-aggregation did occur, even for only a fraction of the silica, the resulting settling rate would be some intermediate value between  $0.022 \text{ s}^{-1}$  (Case A) and  $0.0035 \text{ s}^{-1}$  (Case B). The fact that Case C’s

settling rate is at the lower limit implies no significant homo-aggregation had occurred.

Based on the above “shallow depth” observations, we can draw two very important conclusions: (1) asphaltene precipitation suppresses the homo-aggregation of silica solids, possibly through formation of steric barriers at the particle surfaces, and (2) all stabilized solids are captured by the asphaltene networks and settle as asphaltene-silica complexes.

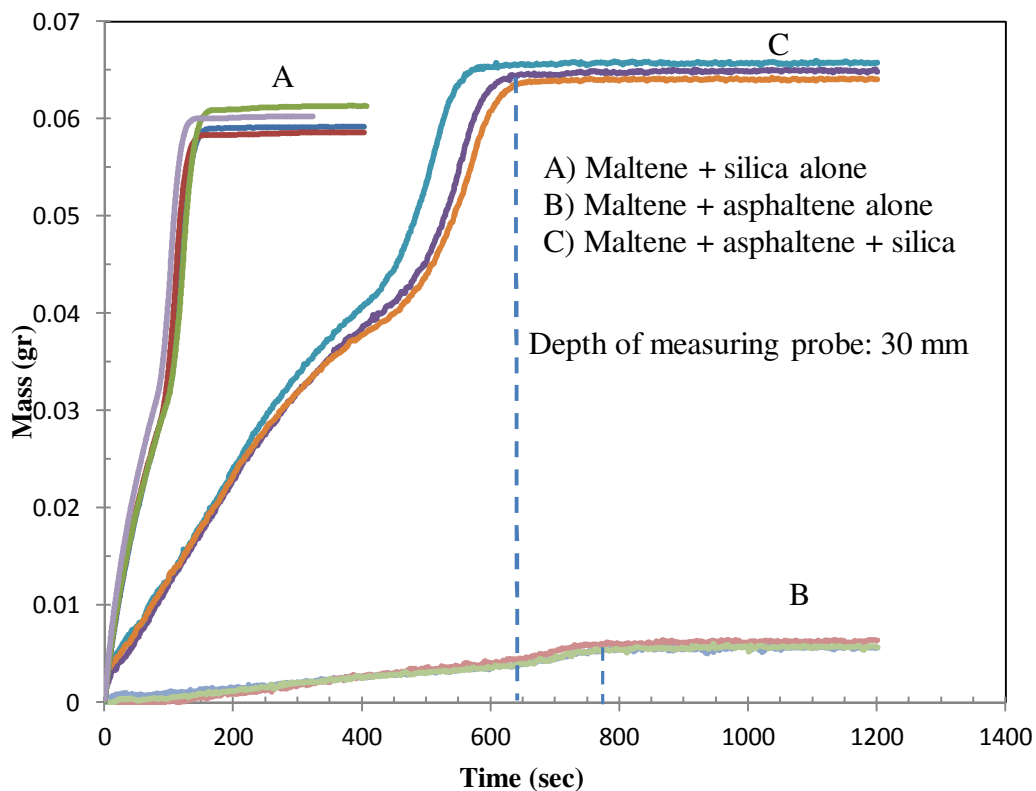


Figure 4.14 The settling curve for Case A) bitumen-coated silica particles in 3 wt. % diluted maltene, Case B) precipitated asphaltenes in 4.5 wt. % diluted bitumen (no silica particle) and Case C) bitumen-coated silica particles in 4.5 wt. % diluted bitumen; collecting tray is located at depth of 30 mm.

Brownian motion is often the dominant mechanism of transport for colloidal particles. As the aggregates grow in size, however, differential settling gradually

becomes the more important transport mechanism. Through differential settling, the asphaltene networks will grow in size and capture more silica particles as they travel downward. This increases the effective density of the asphaltene-silica complexes, and they will settle faster as a result (faster in comparison to asphaltene networks that are devoid of silica solids). This effect should become more apparent at greater depths. Figure 4.14 shows the settling curves for Cases A, B and C — with all conditions the same as before except for the depth of the collecting tray, which was lowered to 30 mm. Similar to Figure 6, we note the significant mass balance between curve C and the sum of steady state masses of curves A and B. Moreover, Curve C, which reflects the settling of the asphaltene-silica complexes, clearly shows a shorter sedimentation time compared to the case with only asphaltene networks (Curve B).

## 5 Summary and recommendation

There are serious environmental concerns related to the current water-based bitumen extraction method. In view of this, development of an alternative method seems to be a necessity. The alternative oil sands extraction method is called “solvent-based,” which uses no water to liberate bitumen from mined ores. Despite its great benefits, there are some unresolved issues with this method, such as the removal of suspended fine particles from the oil phase (i.e. diluted bitumen) before it can be sent to upgrading facilities. This study is motivated by the need to eliminate fine particles from diluted bitumen; the intention is to look into conditions under which fine solid particles can be separated and removed from the oil medium.

Here, micron-sized bitumen coated silica particles were used to simulate the suspended fines in a real extraction process. The hydrocarbon medium was made of different volume ratios of toluene and heptane to allow different degrees of aromaticity. In this study, sedimentation tests were performed on bitumen-coated silica particles in different hydrocarbon media using a sedimentation balance device. For our preliminary experiments, the hydrocarbon media were pure solvents of variable toluene-to-heptane ratios. The settling of solid particles in pure solvent (with no presence of bitumen except for the particle coatings) was studied closely. Strong correlation between solids settling rates and solvent aromaticity was observed (see Section 4.5). These tests were then followed by adding maltene (i.e. de-asphalted bitumen) at mass ratio of 3 wt%, and then

bitumen with mass ratio 5 wt%, to the system. These diluted bitumen solution is used as a more realistic approximation to the hydrocarbon encountered in a real froth treatment operation. For hydrocarbon phases that contained maltenes, the particle settling rate measurements showed there was a strong dependency of settling rates on solvent aromatic content, but the presence of maltene (de-asphalted bitumen) altered the settling rate. Here, the settling rate is an indicator of aggregation and sedimentation.

Particles settling measurement was the main focus of this study. The settling rate is the observable parameter that indicates the amount of aggregation. It also shows how a solvent's aromatic content affects solids removal. The settling rate results explained adhesive forces between micron-sized particles in organic solvents, which could give insight into the mechanism behind the paraffinic froth treatment (PFT) process. However, the focus of this study is not on asphaltene precipitation; it is on the sedimentation and separation of colloidal silica in diluted bitumen. For simplicity, we focus on situations where the diluting solvent is *n*-heptane. We investigated how precipitation of asphaltenes affects the homo-aggregation of silica. The settling rates of silica alone, asphaltenes alone — both in heptane-diluted maltene solutions of the same maltene content — were compared to settling rates of silica in heptane-diluted bitumen.

This finding is evidence for homo-aggregation of particles amongst themselves in *n*-heptane. However, it was observed that the presence of asphaltene precipitates interferes with the homo-aggregation mechanism. Asphaltene precipitates act as steric barriers and suppresses the homo-aggregation of solids. Instead, all

stabilized solids are captured by the asphaltene networks and settle as asphaltene-silica complexes.

For future work, it is recommended that one studies more fully the role of asphaltenes in fine solids removal (from a non-aqueous environment); this can be done by conducting settling experiments of bitumen-coated clay (i.e. kaolinite, illite) particles in de-asphalted bitumen of different sizes. Comparing these results with our findings could provide better understanding of the mechanism of the paraffinic froth treatment process.

## 6 References:

- [1] Anonymous, “Worldwide look at reserves and production,” *Oil Gas J*, pp. 4–5, 2013.
- [2] Masliyah, J., Czarnecki, And, Z., and Xu, *Handbook on Theory and Practice of Bitumen Recovery from Athabasca Oil Sands. Vol. 1: Theoretical Basis*. Kingsley, 2011.
- [3] M. Woynillowicz, D., Severson-Baker, C. & Raynolds, *Oil Sands Fever: The Environmental Implications of Canada’s Oil Sands Rush*, no. November. Pembina institute, 2005.
- [4] O. P. Strausz and E. Lown, *The Chemistry of Alberta Oil Sands, Bitumen and Heavy Oils*. Alberta Energy Research Institute, 2003.
- [5] Y. Xu, T. Dabros, and H. Hamza, “Study on the Mechanism of Foaming from Bitumen Froth Treatment Tailings,” *J. Dispers. Sci. Technol.*, vol. 28, no. 3, pp. 413–418, Mar. 2007.
- [6] B. J. Grant, E. Angen, and S. Dyer, “Forecasting the impacts of oilsands expansion with each barrel of bitumen production,” vol. m, pp. 1–13, 2013.
- [7] B. D. Sparks and F. W. Meadus, “A Combined Solvent Extraction and Agglomeration Technique for the Recovery of Bitumen from Tar Sands,” *Energy Process. Canada*, pp. 55–61, 1979.
- [8] B. D. Sparks and F. W. Meadus, “A Study of Some Factors Affecting Solvent Losses in the Solvent Extraction-Spherical Agglomeration of Oil Sands,” *Fuel Process. Technol.*, pp. 251–264, 1981.
- [9] F. W. Meadus, P. J. Chevrier, and B. D. Sparks, “Solvent Extraction of Athabasca Oil Sand in a Rotating Mill; Part 1 Dissolution of Bitumen,” *Fuel Process. Technol.*, vol. 6, pp. 277–287, 1982.
- [10] F. W. Meadus, B. P. Bassaw, and B. D. Sparks, “Solvent Extraction of Athabasca Oil Sand in a Rotating Mill; Part 2 Solids-Liquid Separation and Bitumen Quality,” *Fuel Process. Technol.*, vol. 6, pp. 289–300, 1982.
- [11] J. R. Farnand, F. W. Meadus, and B. D. Sparks, “Removal of Intractable Fine Solids From Bitumen Solutions Obtained by Solvent Extraction of Oil Sands,” *Fuel Process. Technol.*, pp. 131–144, 1985.

- [12] B. D. Sparks, F. W. Meadus, A. Kumar, and J. R. Woods, "The Effect of Asphaltene Content on Solvent Selection for Bitumen Extraction by the SESA Process," *Fuel*, vol. 1349–1353, 1992.
- [13] E. O. Sparks, B.D., Meadus, F.W. & Hoefele, "Solvent Extraction Spherical Agglomeration of Oil Sands," *Environ. Int.*, 1988.
- [14] C. R. Hsieh and R. K. Clifford, "Solvent Extraction Process for Recovering Bitumen from Tar Sand," 4,676,8891987.
- [15] W. E. Savage and H. A. Cheney, "Process for Solvent Extraction of Bitumen from Oil Sand," 3,553,0991971.
- [16] D. N. Madge and W. N. Garner, "Theory of asphaltene precipitation in a hydrocarbon cyclone," *Miner. Eng.*, vol. 20, no. 4, pp. 387–394, Apr. 2007.
- [17] Y. Jin, W. Liu, Q. Liu, and A. Yeung, "Aggregation of silica particles in non-aqueous media," *Fuel*, vol. 90, no. 8, pp. 2592–2597, Aug. 2011.
- [18] M. Rhodes, *Introduction to particle Technology*, Second Edi. Wiley, 2008, pp. 1–26.
- [19] W. R. Elimelech M, Gregory J, Jia X, *Particle deposition and aggregation: measurement, modelling and simulation*. Elsevier, 1995.
- [20] R. Bürger and W. L. Wendland, "Sedimentation and suspension flows : Historical perspective and some recent developments," pp. 101–116, 2001.
- [21] G. J. Kynch, "A THEORY OF SEDIMENTATION," *Trans. Faraday Soc.*, vol. 48, pp. 166–176, 1952.
- [22] G. H. Coe, H.S. , Clevenger, "Methods for determining the capacities of slime-settling tank," *Trans. AIME*, 1916.
- [23] J. R. Richardson, J. F., Harker, J. H., and Backhurst, "Sedimentation," in in *Coulson and Richardson's CHEMICAL ENGINEERING Particle Technology and Separation Processes*, 5th ed., Coulson and Richardson's Chemical Engineering, 2002.
- [24] D. H. Woodward, "SEDIMENTATION OF MONODISPERSE POLYSTYRENE LATEX," vol. c, pp. 238–244, 1964.
- [25] C. P. Johnson, X. Li, and B. E. Logan, "Settling Velocities of Fractal Aggregates," *Environ. Sci. Technol.*, vol. 30, no. 6, pp. 1911–1918, Jan. 1996.

- [26] K. H. Gardner, T. L. Theis, and T. C. Young, "Colloid aggregation: numerical solution and measurements," *Colloids Surfaces A Physicochem. Eng. Asp.*, vol. 141, no. 2, pp. 237–252, Nov. 1998.
- [27] E. . Gonzalez and P. . Hill, "A method for estimating the flocculation time of monodispersed sediment suspensions," *Deep Sea Res. Part I Oceanogr. Res. Pap.*, vol. 45, no. 11, pp. 1931–1954, Nov. 1998.
- [28] "Particle aggregation," 2012. [Online]. Available: [http://en.wikipedia.org/wiki/Particle\\_aggregation](http://en.wikipedia.org/wiki/Particle_aggregation). [Accessed: 20-Jan-2014].
- [29] J. Gregory and C. R. O. Melia, "Critical Reviews in Environmental Control Fundamentals of flocculation," *Crit. Rev. Environ. Control*, vol. 19, no. 3, pp. 185–230, 1989.
- [30] S. Masliyah, J., Bhattacharjee, *Electrokinetic and Colloid Transport Phenomena*. JohnWiley & Sons, Inc, 2006.
- [31] J. N. Israelachvili, *Intermolecular and Surface Forces Third Edition*. Elsevier Inc, 2011.
- [32] V. der Hoeven, "Electrostatic stabilization in nonaqueous media," *Adv. Colloid Interface Sci.*, vol. 42, pp. 205–277, 1992.
- [33] H. Butt, K. Graf, and M. Kappl, *Physics and Chemistry of Interfaces*. WILEY-VCH GmbH & Co, 2003.
- [34] O. C. Mullins, E. Y. Sheu, A. Hammami, and A. G. Marshall, *Asphaltenes, Heavy Oils, and Petroleomics*. Springer Science, 2007.
- [35] S. D. Taylor, J. Czarnecki, and J. Masliyah, "Refractive index measurements of diluted bitumen solutions," vol. 80, no. 2001, pp. 2013–2018, 2013.